

LOCAL SHELL-SIDE HEAT TRANSFER COEFFICIENTS  
IN THE VICINITY OF BAFFLES IN  
TUBULAR HEAT EXCHANGERS

by

MYSORE SHAMANNA GURUSHANKARIAH

A THESIS

submitted to

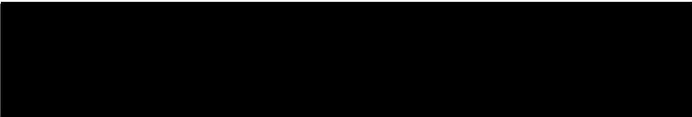
OREGON STATE COLLEGE


in partial fulfillment of  
the requirements for the  
degree of


MASTER OF SCIENCE


June 1958

APPROVED:

  
\_\_\_\_\_  
Professor of Chemical Engineering  
In Charge of Major

  
\_\_\_\_\_  
Head of Department of Chemical Engineering

  
\_\_\_\_\_  
Chairman of School Graduate Committee

  
\_\_\_\_\_  
Dean of Graduate School

Date thesis is presented February 8, 1958

Typed by Maritza A. Bodine

## ACKNOWLEDGEMENT

The writer takes this opportunity to make the following acknowledgements:

To The National Science Foundation for the granting of a fellowship to conduct the present research.

To Dr. J. G. Knudsen for his suggestion of the problem and procurement of the research grant and for his inspiring encouragement and guidance through out the duration of this investigation.

To Mr. R. C. Mang, departmental machinist, for his assistance in repairs to the equipment.

To the Department of Chemical Engineering for the use of its facilities and equipment.

To Mr. D. E. Amos for his assistance in programming for the digital computer.

To the Department of Mathematics for the use of the digital computer.

## TABLE OF CONTENTS

Section		Page
I	Introduction . . . . .	1
II	Review of Literature . . . . .	4
	1. Heat Transfer Normal to Single Cylinders . . . . .	7
	2. Heat Transfer Normal to Tube Banks . . . . .	8
	3. Baffled Tubular Heat Exchangers . . . . .	9
	(a) Resistance to Heat Flow in Heat Exchangers . . . . .	10
	(b) Effects of Shell-Side Geometry on the Shell-Side Heat Transfer rates . . . . .	13
	(c) Analysis of Shell-Side Flow . . . . .	16
	(d) Shell-Side Heat Transfer Coefficients . . . . .	19
	4. Methods of Determining Local Heat Transfer Coefficients. . . . .	23
III	Experimental Equipment . . . . .	25
	1. The Model Heat Exchanger . . . . .	25
	2. The Sensing Probe . . . . .	25
	3. The Air Source and Cooling System . . . . .	33
IV	Experimental Program . . . . .	35
	1. Investigation Positions . . . . .	35
	2. Baffle Spacings . . . . .	36
	3. Flow Rate . . . . .	38
	4. Thermocouple and Tube Numbering System . . . . .	38
V	Experimental Procedure . . . . .	40
VI	Calculation of Data . . . . .	43



## TABLE OF CONTENTS (Continued)

Section		Page
VII	Analysis of Data . . . . .	47
	1. Presentation of Data . . . . .	47
	2. Correlation of Data . . . . .	47
	3. Comparison with measurements of Ambrose . . . . .	58
	4. Discussion of Data . . . . .	60
	(a) Effect of Baffle Spacing . . . . .	60
	(b) Effect of Flow Rate . . . . .	61
	(c) Effect of Clearance Between Tube and Baffle hole . . . . .	62
	(d) Flow Pattern . . . . .	62
	(e) Variation of Heat Transfer Rate Along Tubes . . . . .	65
	(f) Variation of Heat Transfer Rate Around Tubes . . . . .	70
	(g) Experimental Errors and Accuracy Attained . . . . .	70
VIII	Conclusions . . . . .	72
	1. Correlation of Data . . . . .	72
	2. Effect of Baffle Spacing . . . . .	73
	3. Effect of Flow Rate . . . . .	73
	4. Flow Pattern . . . . .	74
	5. Heat Transfer Rate Along Tubes . . . . .	75
	6. Heat Transfer Rate Around a Tube . . . . .	75
IX	Recommendations . . . . .	76
X	Nomenclature . . . . .	77
XI	Bibliography . . . . .	80
Appendix		

# LIST OF TABLES

Table		Page
1	Dimensions of Heat Exchanger Components .....	26
2	Baffle Arrangements and Positions Investigated Along Tubes .....	37
3	Calculated Data for Correlation .....	90
4	Calculated Flow Rates .....	91
5	Calculated Flow Rates .....	93
6	Variation of Average Nusselt Numbers with Flow Rate .....	95
7	Effect of Baffle Hole Clearance .....	96
8	Average Nusselt Numbers in the Various Zones .....	97

## LIST OF FIGURES

Figure		Page
1	Flow Zones in a Heat Exchanger with Segmental Baffles . . . . .	17
2	Model Heat Exchanger and Associated Equipment	27
3	Tube Bundle . . . . .	28
4	Drawing of Assembled Sensing Probe . . . . .	30
5	Diagram of emf Metering System . . . . .	31
6	Wiring Diagram for Power System . . . . .	32
7	Air Flow System . . . . .	34
8	Differential Length of Ribbon . . . . .	46
9	Correlation of Shell-Side Heat Transfer Data	57
10	Comparison of Average Nusselt Numbers with Measurements Made by Ambrose . . . . .	59
11	Graphical Presentation of Data System . . . . .	48
12	Local Shell-Side Heat Transfer Data in a Baffled Tubular Heat Exchanger . . . . .	49
13	Local Shell-Side Heat Transfer Data in a Baffled Tubular Heat Exchanger . . . . .	50
14	Local Shell-Side Heat Transfer Data in a Baffled Tubular Heat Exchanger . . . . .	51
15	Local Shell-Side Heat Transfer Data in a Baffled Tubular Heat Exchanger . . . . .	52
16	Local Shell-Side Heat Transfer Data in a Baffled Tubular Heat Exchanger . . . . .	53
17	Local Shell-Side Heat Transfer Data in a Baffled Tubular Heat Exchanger . . . . .	54

## LIST OF FIGURES (Continued)

Figure		Page
18	Average Nusselt Numbers Along Tubes . . . . .	66
19	Average Nusselt Numbers Along Tubes . . . . .	67
20	Schematic Diagram of Flow Pattern . . . . .	69
21	Variation of Average Nusselt Numbers with Flow Rate . . . . .	87

LOCAL SHELL-SIDE HEAT TRANSFER COEFFICIENTS  
IN THE VICINITY OF BAFFLES IN  
TUBULAR HEAT EXCHANGERS

SECTION I

INTRODUCTION

Heat transfer is an important unit operation in most industrial processes and in most cases heat must be transferred from one flowing fluid to another. For this purpose baffled heat exchangers are commonly used. In designing heat exchangers the engineer encounters difficulty in shell-side heat transfer coefficients owing to shortage of fundamental information on the fluid flow patterns and their associated effect on heat transfer rates. The available information concerns average or overall values useful for the design of similar heat exchangers but becomes insufficient to design a completely new type. In other words, very little of the dynamics of the fluid or the heat is known so that a more fundamental approach to the design problem, other than the empirical method is not possible.

The shell-side heat transfer coefficient depends on the geometry and dimensions of the exchanger such as baffle type, baffle spacing, baffle size, tube size,

tube spacing and the various clearances between the parts of the exchanger. The most common type of baffle is the segmental baffle or half moon baffle with a baffle cut of 25 per cent of baffle diameter. Other types of baffles are the orifice baffle and the disk and doughnut baffle.

A decrease in baffle spacing causes an increase in the local velocities and the number of passes across the tube bank and consequently the heat transfer coefficients increased. Effect of tube size and tube spacing are difficult to separate as the effectiveness of a tube is dependent on the clearance between the tubes. For the same size tubes an increase in tube spacing causes the heat transfer rate to increase. An increase in the clearance between the shell and baffle and between tube and baffle decreases the heat transfer rate. Some exploratory research with a view to investigate these effects and to detect the flow pattern by evaluating the local heat transfer rates was done by Ambrose (1,p.1-183). This work showed that addition of baffles and an increase of tube spacing both caused an increase in heat transfer rate. Between the baffles, a cross flow, longitudinal and eddy flow zone were detected. The effect of baffles was conclusively demonstrated along a tube in the

exchanger by the large values in the baffle holes and moderate values in the baffle window.

The present investigation was undertaken to confirm the findings of Ambrose (1,p.114) and to make a more thorough study of the variation of heat transfer rates along the tubes. The work was done with the same apparatus as Ambrose used. Local heat transfer rates for two baffle spacings and three flow rates were studied between the central two baffles and three fourth inch intervals.

From this study it was possible 1) to correlate the results with literature values, 2) to compare with the results of Ambrose (1,p.114), 3) to study the effect of baffle spacing, 4) to study the effect of flow rate, 5) to detect the flow pattern on the shell-side of the model heat exchanger by studying the variation of heat transfer rates around and along the tubes. To make the results more easily interpreted, the data are presented in picture form.

## SECTION II

## REVIEW OF LITERATURE

The unit operation of heat transfer is encountered in most industrial processes and has been investigated extensively by engineers and scientists alike. The mechanism of heat transfer is fairly well known but still there are many aspects of it that need further study.

There are three ways to transfer heat: Conduction, convection and radiation. Of these convection is most important for transfer of heat between two fluids.

The rate of heat transfer by conduction is proportional to the surface area and the temperature gradient.

$$q = k A \Delta t \quad (1)$$

where

$q$  = rate of heat transfer

$A$  = area transferring heat

$t$  = temperature gradient

$k$  = proportionality constant

This proportionality constant for this equation is the thermal conductivity  $k$ . This can also be thought of as a measure of the resistance to flow of heat.



The rate of heat transfer by convection is proportional to the surface area and to the temperature difference between the surface and the bulk of the fluid.

$$q = h A (t_s - t_f)$$

where

$q$  = rate of heat transfer

$A$  = area transferring heat

$(t_s - t_f)$  = temperature difference between surface and fluid

$h$  = proportionality constant

This proportionality constant is called the heat transfer coefficient and this equation is analogous to the equation for conduction.

The rate of heat transfer by radiation is proportional to the surface area and to the fourth power of the temperature. The heat transfer equation is also analogous to the other two equations discussed above.

Forced convection is widely employed in industrial processes where heat must be transferred from one fluid to the other. Heat exchangers are used for this purpose.

In forced convection the resistance to heat

flow is greatly influenced by the flow characteristics of the system. For this reason the mechanism of fluid flow close to a heating or cooling surface is of primary importance from a heat transmission standpoint.

As a fluid in turbulent motion flows past a solid boundary three types of flow occur near the boundary, the layer in direct contact with the surface is in laminar motion. It is called the laminar sublayer. Evidence of existence of this layer was demonstrated by Couch and Herrstrom (\*) by an undisturbed color band at the surface. Bordering the laminar sublayer is a buffer zone consisting of both laminar and turbulent flow. It is a general belief that the thickness of the buffer layer varies with time because of the more or less periodic formation of vortices ( 22, p. 152). Beyond the buffer zone the flow is turbulent and is characterized by a flow stream made up of a large number of eddies and of particles in chaotic motion.

Transference of heat takes place from the surface to the laminar layer by molecular conduction. In the buffer zone and turbulent core, heat is transferred mainly by mixing of the particles with molecular conduction playing a very minor role. The laminar layer therefore offers the major resistance to flow of heat. The resistance of the buffer layer varies inversely as the turbulence.

\* Quoted in McAdams (22, P. 152)

The bulk stream has very little resistance. To increase the heat transfer rate the thickness of the laminar layer is reduced by increasing the bulk fluid velocity or turbulence.

### 1. Heat Transfer Normal to Single Cylinders

The variation of tube to fluid heat transfer coefficients around a single cylinder tube placed normal to a flowing stream has been studied at length (13, p. 375-381), (37, p. 1-79), (31, p. 177-180), and (36, p. 1087-1093). A comparison of the data obtained by these investigators is in generally in agreement. A plot of the Nusselt number  $\frac{hd}{k}$  versus the angle measured from the leading edge gives two types of curves. In one type of curve the Nusselt number decreases from the leading edge to a minimum in the range of 80 to 105 degrees and then increases again. In the other type, the variation of the Nusselt number is similar except that it shows two minimums, one in the 80 to 105 degrees range and another at 130 degrees. The second type curve occurs at a Reynolds number of  $5 \times 10^4$  at low turbulence or beyond  $5 \times 10^4$  at high turbulence.

A laminar boundary layer forms on the cylinder at the leading edge and increases in thickness up to 80 or 105 degrees. In this vicinity the boundary layer

separates causing a minimum Nusselt number. In the second type of curve at high Reynolds numbers and high turbulence the boundary layer becomes turbulent before it separates. The first minimum is the point of transition of laminar to turbulent flow in the boundary layer. The second minimum is the point of separation.

Levy (21, p. 341-348) has calculated local heat transfer coefficients along submerged bodies in terms of several parameters for specific Prandtl numbers. The following empirical relationship has been obtained from the data of Schmidt and Wenner (26, p. 1-15) for the prediction of local Nusselt numbers around cylindrical tubes in cross flow.

$$Nu = 1.14 (Re)^{0.5} (Pr)^{0.4} \left[ 1 - \left( \frac{\theta}{90} \right)^3 \right] \dots\dots (3)$$

where

Nu = Nusselt number

Re = Reynolds number

Pr = Prandtl number

$\theta$  = the angle measured from the leading edge

This equation holds for angles up to 80 degrees and Reynolds numbers less than  $5 \times 10^5$ .

## 2. Heat Transfer Normal to Tube Banks

Considerable research has been done in order to understand the mechanism of heat transfer and flow of

fluids across banks of tubes. Common variables affecting the rate of heat transfer are tube size, tube spacing, tube arrangement, types of fluid and fluid flow rate.

Usually the tubes are arranged in one of two ways:

(1) square or inline pitch, or (2) triangular or staggered pitch.

The staggered arrangement gives substantially higher heat transfer coefficients than the inline arrangement (22, p. 271) as demonstrated by the investigators of Bergelin, et al. (2, p. 955), (17, p. 387-896), (14, p. 583-594), (30, p. 11-20), (11, p. 1-15). The results of these workers indicate that the first row of tubes has a Nusselt number which is about 40 per cent below the average for the whole bank. The Nusselt number increases from the first row to a maximum at the third row, decreases slightly at the fourth row and stays essentially constant for all following rows.

### 3. Baffled Tubular Heat Exchangers

Baffled tubular heat exchangers are widely used in industry where heat transfer by forced convection between two fluids is desired. Such exchangers consist of a tube bundle located inside a shell, with one fluid flowing inside and the other flowing across the tubes. In the design of a heat exchanger it is necessary to know the

various resistances to heat flow the effect of structural features and dynamics of flow of the fluids.

(a) Resistance to Heat Flow in Heat Exchangers

Fourier's law (12) for unidirectional conduction of heat states mathematically

$$\frac{dq}{d\theta} = - k A \frac{dt}{dx} \quad (4)$$

where

$\frac{dq}{d\theta}$  = differential rate of heat transfer per time

$k$  = thermal conductivity

$A$  = area of heat transfer

$\frac{dt}{dx}$  = temperature gradient along the path of heat transfer

For steady state, the equation becomes

$$\frac{dq}{dA} = - k \frac{dt}{dx} \quad (5)$$

on integrating it becomes

$$q = \frac{\Delta t}{x/kA_m} = \frac{\Delta t}{R} \quad (6)$$

therefore

$$R = \frac{x}{kA_m} \quad (7)$$

where

$R$  = the resistance

$A$  = mean area

For the case of convection the heat transfer equation is modified as

$$q = h A \Delta t \quad (8)$$

where

$h$  = Coefficient of heat transfer from surface to fluid

So the resistance  $R$  in this case will be

$$R = \frac{1}{hA} \quad (9)$$

These reciprocal resistances or conductances are additive.

Considering that the heat is flowing from the shell-side fluid to the fluid inside the tubes, the following resistances are encountered: Shell-side film (laminar layer close to the tube surface); Shell-side deposit or scale; metal tube; and the tube side film. When the thickness of the tube is small compared to its diameter, the following equation may be derived as described above

$$\frac{1}{U} = \frac{1}{A_s h_s} + \frac{1}{A_s h_{ds}} + \frac{x_w}{A_{av} K_w} + \frac{1}{A_t h_{dt}} + \frac{1}{A_t h_t} \quad (10)$$

where

$h_s$  = film heat transfer coefficient of shell-side fluid

$h_{ds}$  = scale deposit heat transfer coefficient on shell-side of tube

$x_w$  = thickness of tube wall

$k_w$  = thermal conductivity of tube material

$h_t$  = film heat transfer coefficient of tube fluid

$h_{dt}$  = scale deposit heat transfer coefficient inside tube

$A_s$  = shell-side area

$A_t$  = tube side area

$A_{av}$  = average of tube and shell-side area

Resistances due to the scales and the tube materials can be evaluated simply. The film heat transfer coefficients for fluids inside tubes can be evaluated from a Colburn type equation (5). This is also given in McAdams (22, p. 219).

$$\frac{hd_1}{k} = 0.023 \left( \frac{d_1 G}{\mu} \right)^{0.8} \left( \frac{C_p \mu}{k} \right)^{0.4} \quad (11)$$

where

$h$  = the film heat transfer coefficient Btu/hr. ft<sup>2</sup>

$d_1$  = the inside diameter of tube in ft.

$k$  = the thermal conductivity of the fluid  
Btu/hr. (sq. ft.)(deg F per ft)

$G$  = the mass velocity lb/hr. (sq. ft)  
the viscosity lb/hr.ft.

$C_p$  = the specific heat of the fluid Btu/lb. deg F.

Evaluation of the shell-side heat transfer coefficients is difficult because of the complexity of the flow pattern on the shell-side. Most data have been correlated by means of empirical equations for a limited number of exchangers variables, as outlined below.



(b) Effects of Shell-Side Geometry on the Shell-Side Heat Transfer Rates

The shell-side heat transfer coefficient for a heat exchanger depends on the geometry of the exchanger and the properties of the fluid. Variables describing the geometry are baffle type, baffle spacing, baffle size, tube spacing and the various clearances between the parts of the heat exchanger.

The types of baffles commonly used are segmental or half-moon baffles, orifice baffles and disk and doughnut baffles. The segmental baffle is the most widely used. For this type of baffle the baffle cut is generally 25 per cent of the inside diameter of the shell. For the same heat transfer rate the pressure drop increases in the following order: disk and doughnut baffle, segmental baffle and the orifice baffle.

Any geometry change which allows the fluid to mix more thoroughly after passing over the heat transfer surface causes an increase in the heat transfer rate. The time required for the flow to progress from one heating surface to the next is referred to as the mixing time.

For a given length of exchanger and a given rate of flow a decrease in baffle spacing increases the heat transfer rate for all the three types of baffles. This is confirmed for the segmental baffle case by the

investigations of Ambrose ( 1, p. 95). This increase in heat transfer rate is attributed to higher local velocities and larger number of passes across the tube bank which more than offset the drop of heat transfer due to decreased mixing time.

A smaller baffle cut in the segmental baffle increases the velocity through the baffle window and also extends the length of cross flow across the bank. This increases the heat transfer coefficient. Donohue (8, p. 2503) Plotted the data of both Short (28, p. 55) and Tinker (33, p. 97-103) for segmental baffles having varying depths of cuts and found that the rate of heat transfer does increase with decreasing baffle cut.

The effect of tube size and tube spacing are difficult to separate as the effectiveness of a tube is dependent on the clearance between tubes. For constant tube clearance and local velocity, a reduction in the tube size results in the increase of heat transfer rate. An increase in the tube spacing also causes an increase in the heat transfer rate ( 27, p. 779-785) and ( 1, p. 99).

The mechanical clearances between the component parts of the exchanger significantly affect the heat transfer rates. Reduction of clearances increase the heat transfer rate but also increase the pressure drop across the exchanger. For an economical design optimum clearances

should be determined to keep the heat transfer rate at a maximum and the power cost at a minimum. The effect of clearances on the heat transfer rate depends on the flow pattern and fluid leakage in the clearance. The significant clearances in a heat exchanger are:

1. The baffle cut or baffle window, the major zone of leakage.
2. The clearance between tube and baffle holes.
3. The clearance between tube bundle and shell.
4. The clearance between baffle and shell.
5. The space between tubes.
6. The space in the unbaffled end zones.

The above clearances are often determined from consideration of factors such as thermal, corrosive, and fouling characteristics of the fluid to be handled; design pressures; means of providing expansion; structural strengths of materials, costs, machinabilities, etc. They are necessary and cause inevitable leakage. It can be stated in general that an increase in the clearance decreases the heat transfer rate and vice-versa except for the clearance between tubes which shows an opposite tendency. These facts are substantiated by the investigations of Donohue (8, p. 2509), Perrone (25, p. 71-72), Tinker (34, p. 110-115) and Ambrose (1, p. 115).

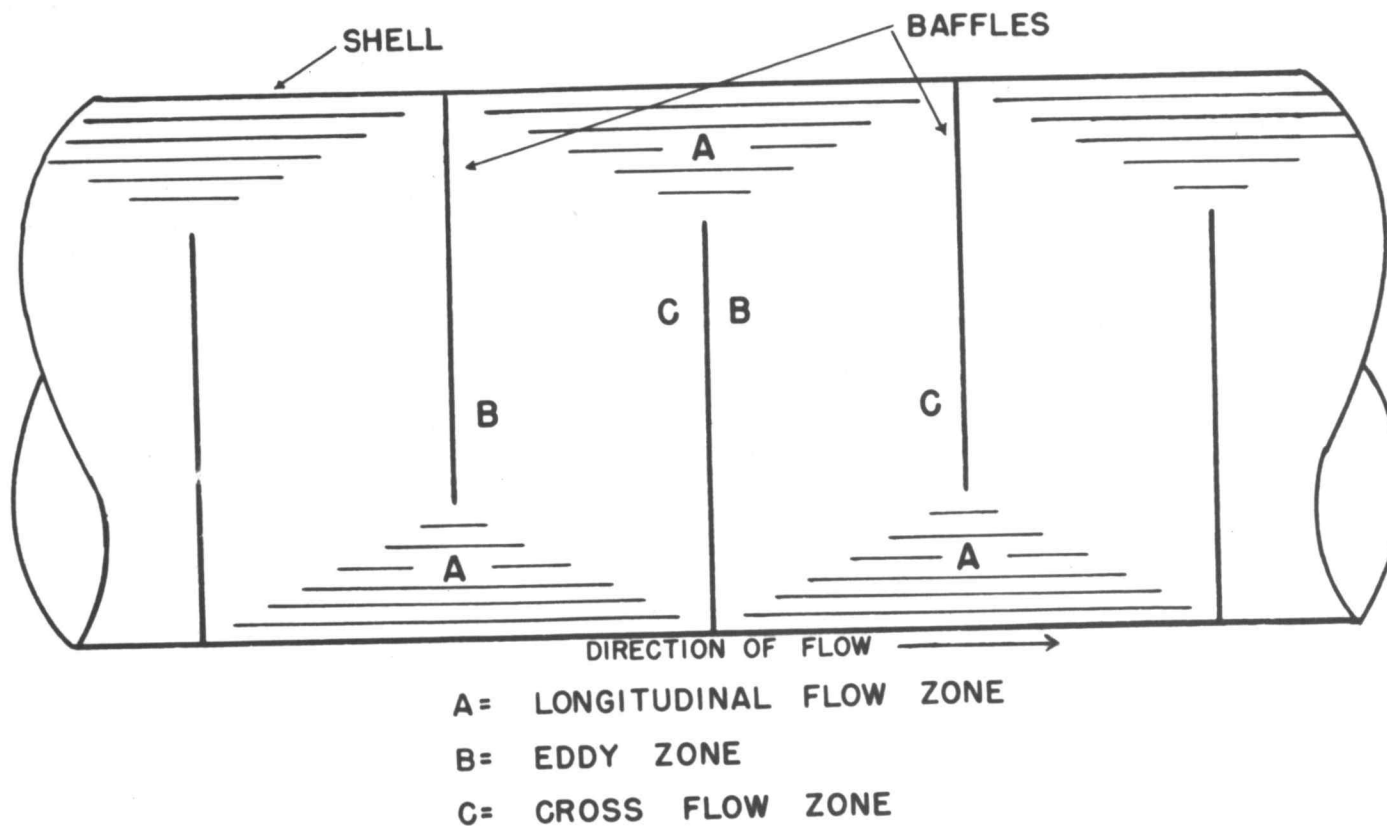
(c) Analysis of Shell-Side Flow

Flow on the shell-side of a heat exchanger is highly complicated. Several workers have attempted to analyze the problem dividing the shell-side into different types of flow zones. Most workers consider only a two-dimensional flow pattern on a central longitudinal cross section of the exchanger and assume the same pattern in a perpendicular direction but there appears to be a pattern in the perpendicular direction also as can be expected in any three-dimensional flow.

Donohue (8, p. 2499-2511) considered the flow in a baffle space in two parts, flow through the baffle window as longitudinal and flow across the tube bundle as cross-flow. This division is shown in Figure 1. A is the longitudinal flow zone and B and C represent the cross-flow zone.

Perrone (25, p. 71-72) made the same division but considered the cross-flow distance to be between the center of gravity of the baffle window and the center of gravity of the next baffle window.

Gupta and Katz (16, p. 998-999) divided the flow in a baffle space into three parts A, B, and C as shown in Figure 1, A is the longitudinal flow zone; B is the eddy flow zone; and C is the true cross-flow zone. These zones were determined by a visual study of colored



FLOW ZONES IN A HEAT EXCHANGER WITH SEGMENTAL BAFFLES  
FIGURE 1

polystyrene beads in the shell side fluid of glass heat 18  
exchanger. This exchanger has no clearance between tubes  
and baffles or between baffles and shell.

Gunter, Sennstrom and Kopp (15) show the flow patterns  
for flow past solid baffles of varying heights and  
spacings. These patterns were obtained by observation  
of fine aluminum powder on the surface of the fluid in a  
two-dimensional system of baffles and exchanger. Even  
in this case there are no clearances other than the baffle  
window. The eddy zones are easily discernible in the  
patterns.

Tinker (32, p. 89-96), (33, p. 97-109), (34, p. 110-  
116) has made a more detailed analysis of the shell-side  
flow. He has taken the leakages due to the various clear-  
ances also into consideration. The flow pattern is  
significantly affected by clearances. He divides the flow  
into five zones:

1. A cross-flow stream through the tube bundle.
2. Orifice leakages through the tube holes.
3. Parallel flow through baffle windows.
4. Flow in regions of transition between parallel  
and cross-flow.
5. By-pass streams around the tube bundle.

These streams are affected by the various clearances  
between the heat exchanger components, and consequently  
the heat transfer rates are affected. An increase in the

19  
tube hole clearance of  $1/64$  inch results in a reduction of the cross-flow heat transfer coefficient by 10 per cent, Tinker (34, p. 110). An increase of  $1/16$  inch of clearance reduces the coefficient by 8 per cent. This however is more for smaller exchangers than large ones.

Complete elimination of shell to tube bundle clearance can result in an increase of cross-flow heat transfer coefficient by as much as 40 per cent, Tinker (34, p. 111).

It is interesting to note that the pressure drop is reduced by increasing the various clearances and the power requirement is lower but for a given heat transfer rate the power requirement for an exchanger with less clearances is less than the exchanger with more clearances.

#### (d) Shell-Side Heat Transfer Coefficients

All the data on shell-side heat transfer have been correlated empirically since the complexity of the flow pattern and paucity of fundamental knowledge of the flow pattern precludes an analytical solution. However if more information on the actual dynamics of the flow is obtained it might be possible to obtain an analytical solution.

The method of correlation depends on modifying the mass velocity of the flow of fluid through the exchanger.

Various investigators have adopted different methods. 20

Donohue (8, p. 2502) determined a weighted mass velocity by taking the geometric mean of the cross-flow mass velocity and the longitudinal mass velocity through the baffle window.

Donohue (8, p. 2504) proposed the following equation for tubular heat exchangers:

$$\frac{hd}{k} = 0.25 \left( \frac{dG_e}{\mu} \right)^{0.6} \left( \frac{C_p \mu}{k} \right)^{0.33} \left( \frac{\mu}{\mu_w} \right)^{0.14} \quad (12)$$

where

$h$  = heat transfer coefficient, Btu/hr. ft.<sup>2</sup> °F

$d$  = outside diameter of tube, ft.

$k$  = thermal conductivity of shell-side fluid,  
Btu/hr. ft.<sup>2</sup> °F/ft.

$G_e$  = weighted mass velocity  $\frac{W}{\sqrt{A_B A_C}}$ , lb/hr. ft.<sup>2</sup>

$W$  = mass rate of flow, lb/hr.

$A_B$  = baffle window area, ft.<sup>2</sup>

$A_C$  = cross-flow area, ft.<sup>2</sup>

$\mu$  = average viscosity of shell fluid, lb/hr. ft.

$\mu_w$  = viscosity of shell fluid at heat exchange surface,  
lb/hr. ft.

$C_p$  = specific heat, Btu/lb. °F.

Williams and Katz (35, p. 26), Bergelin, et al.

(3, p. 841) and Ambrose (1, p. 89-94) used the same type of analysis in their correlation work.

Short (28, p. 6) used an average mass velocity which



consisted of three equally weighted parts:

1. Mass velocity through the baffles.
2. Mass velocity through minimum area perpendicular to tubes.
3. Mass velocity through the maximum area perpendicular to tubes.

He used the following equation for segmental baffled exchangers:

$$\frac{hd}{k} = 15.8 \left( \frac{C_p \mu}{k} \right)^{0.32} \left( \frac{P-d}{P} \right)^{0.5} \left[ dG_s \left( \frac{B}{L} \right)^{1.72} \right]^{0.6} \left[ \left( \frac{d}{D} \right)^{0.86} \left( \frac{L}{S} \right)^{0.55} \right]^{0.6} \quad (13)$$

where

P = tube pitch, ft.

$G_s$  = mass flow rate in shell without baffles,  
lb/hr. ft.<sup>2</sup>

L = active length of exchanger, ft.

B = baffle height, ft.

S = baffle spacing, ft.

and the rest have the usual significance.

Kern (18, p. 137) has used the equation

$$\frac{hoDe}{k} = 0.36 \left( \frac{De G_s}{\mu} \right)^{0.55} \left( \frac{C \mu}{k} \right)^{1/3} \left( \frac{\mu}{\mu_w} \right)^{0.14} \quad (14)$$

where

ho = heat transfer coefficient for outside fluid,  
Btu/hr. ft.<sup>2</sup> °F.

$D_e$  = equivalent diameter for heat transfer and pressure drop, ft.

$k$  = thermal conductivity, Btu/hr. ft.<sup>2</sup> °F/ft.

$G_s$  = shell-side mass velocity, lb/hr. ft.<sup>2</sup>

$\mu$  = viscosity, lb/hr. ft.

$\mu_w$  = viscosity at tube-wall temperature, lb/hr. ft.

$\mu$  = viscosity, lb/hr. ft.

$C$  = specific heat of fluid, Btu/lb. °F.

He indicates that a plot of the above equation for the test data of Breidenbach and O'Connell (4, p. 761-776) agrees very well with the methods of Colburn (5, p. 174-210) and Short (27, 779-785). Tinker (32, p. 89-96) evaluated the effective area of flow by using correction factors. This effective area was used to calculate the effective Reynolds number. A cross-flow coefficient was calculated by multiplying the total heat transfer coefficient by the effective area. This cross-flow coefficient was used in the calculation of the Nusselt number. He made a log-log plot of the dimensionless term  $Nu(Pr)^{-1/3} \left( \frac{\mu}{\mu_w} \right)^{-0.14}$  versus the effective Reynolds number and obtained a good correlation for 11 different baffled oil coolers.

It can be seen in all these correlations that the average shell-side heat transfer coefficients are evaluated from experimental data and use is made of a modified mass velocity to correlate them but this approach

nothing about the actual dynamics of heat or fluid flow. Hence, it is apparent that more knowledge of the flow pattern and its effect on the local heat transfer rates is necessary to make a more fundamental approach to this problem. Ambrose (1) made a step in this direction but extensive work needs to be done.

#### 4. Methods of Determining Local Heat Transfer Coefficients

Several methods have been used to determine local heat transfer coefficients, each of which has some advantages and some disadvantages. Of the several methods mention may be made of Thomson, et al. (31, p. 177-178), Schmidt and Wenner (26, p. 2-4), Zapp (37, p. 23-26), Dwyer, et al. (11, p. 5-7), Geidt (13, p. 375-377), and the sublimation of naphthalene method. A detailed discussion of these methods was made by Ambrose (1, p. 26-31) and he came to the conclusion that Geidt's method is very well suited to this type of study on the following considerations:

1. Ability to measure temperatures at close intervals is necessary.
2. Necessity of an isothermal surface is not desirable.
3. Easy transference of the measuring device from

position to position and maintenance of the shape of the device are desirable.

4. A short response time is a necessary feature.

These considerations were very well satisfied by the resistance heating technique used by Geidt (13, p. 376-377).

## SECTION III

## EXPERIMENTAL EQUIPMENT

The heat exchanger apparatus shown in Figure 2, was fabricated and used by Ambrose. The same apparatus was used in the present work. It consisted mainly of a model heat exchanger, a sensing probe, a direct current power source, an emf measuring arrangement and an air source.

## 1. The Model Heat Exchanger

The exchanger was 45-inches long. The six-inch diameter shell was made of lucite plastic tube. The tube bundle was made up of fourteen one-inch aluminum condenser tubes, steel tie-rods, and plastic baffles and tube sheets. Figure 3 shows the tube bundle. The shell had an entrance and an exit for air at right angles to the axis of the exchanger. The baffles were 1/8-inch thick plastic sheets. The dimensions of the shell, tubes and baffles are shown in Table 1.

## 2. The Sensing Probe

The sensing probe could measure the temperature at any point along or around a tube, from which measurements the local heat transfer coefficients could be calculated.

TABLE I

26

## Dimensions of Heat Exchanger Components

Exchanger Shell

Inside diameter	5.710 - 0.03 inches
Outside diameter	5.937 - 0.03 inches
Length	45.00 inches

Baffles

Baffle diameter	5.594 - 0.002 inches
Height at Cut	4.290 - 0.002 inches
Drilled Holes	1.063 - 0.010 inches

Tubes

Outside Diameter	1.000 - 0.001 inches
------------------	----------------------

Drilled Holes

Tube Holes in Tube Sheets	1.000	0.003 inches
Tie-Rod Holes	3/16	inch
Flange-Tube Sheet Bolt Holes	1/4	inch

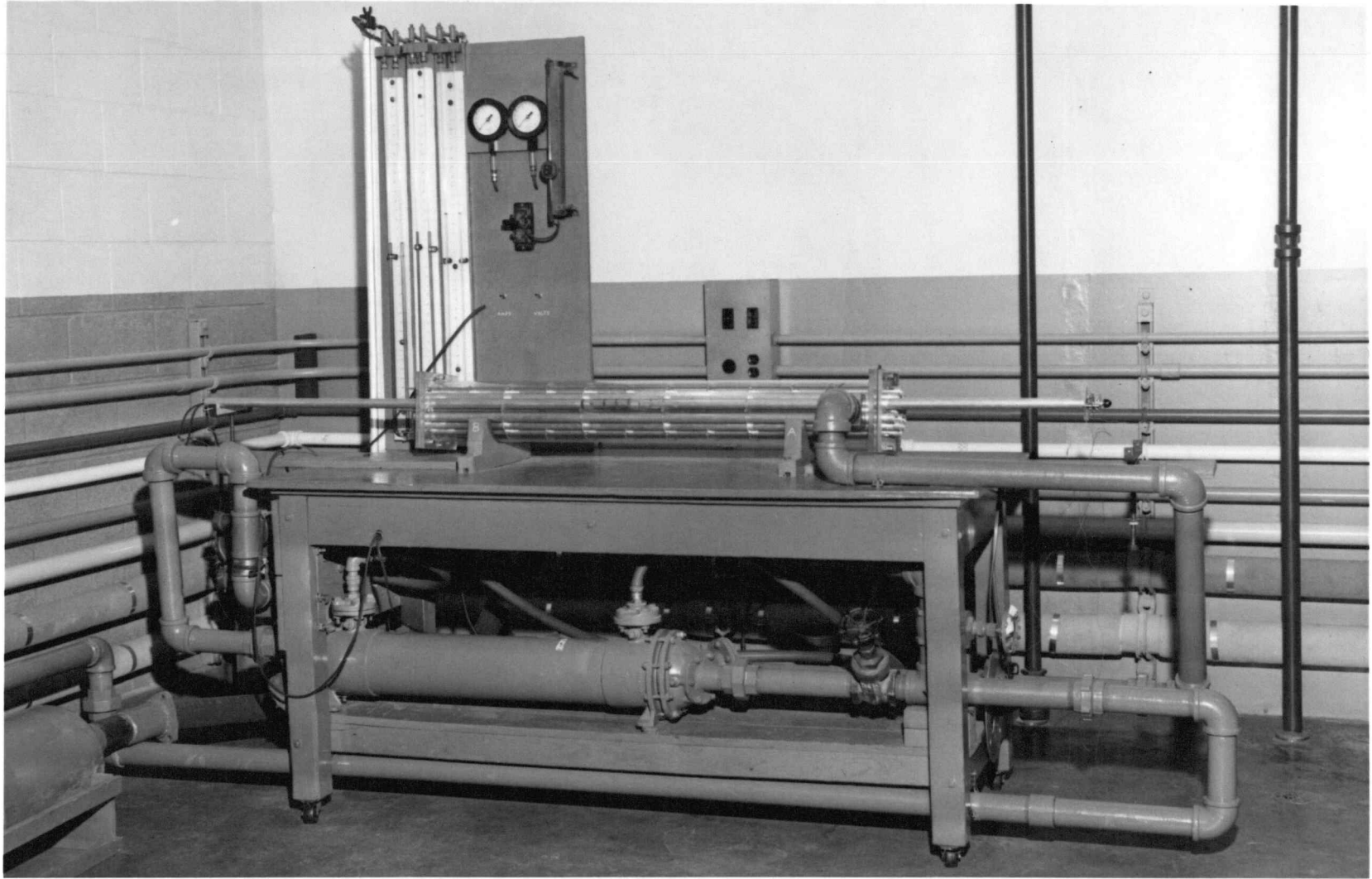


Figure 2 Model Heat Exchanger and Associated Equipment

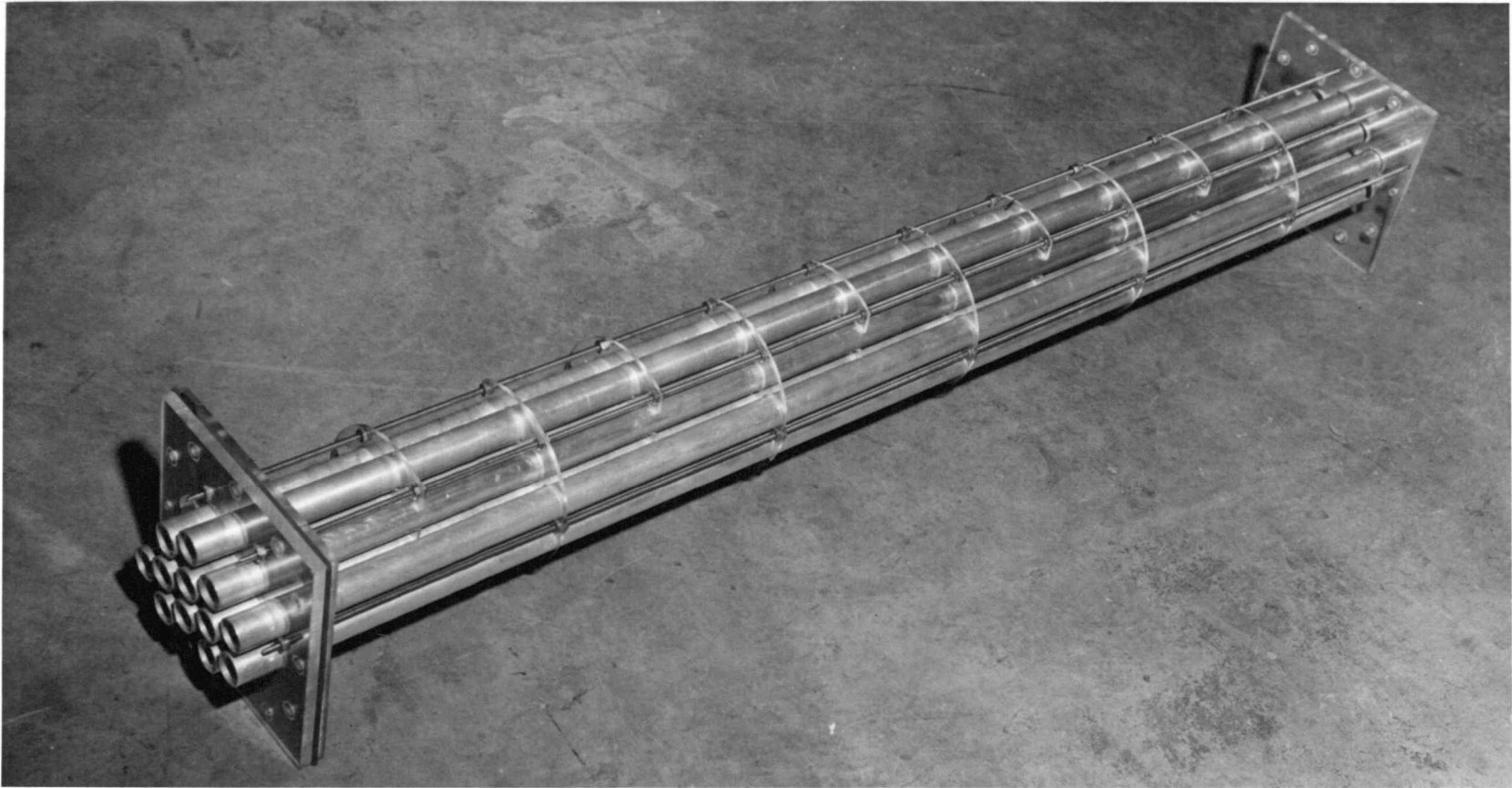


Figure 3 Tube Bundle



The probe could be moved from one location to the other. Three one-inch wide by 0.002 inch thick pieces of Trophet C resistance ribbons were wrapped around a plastic bar as shown in Figure 4. The Trophet C resistance ribbon had a resistance of 0.271 ohm per foot and a thermal conductivity of 7.63 Btu/Hr. Ft.<sup>2</sup> °F/Ft. Electric power was supplied to these ribbons by copper bars which also held them in position. Seven iron-constantan thermocouples were located in a groove under the center ribbon and insulated from the ribbon by a layer of "Saran Wrap". Thermocouple leads entered from a multiple junction selector switch at the upstream end and the power leads from the opposite end. The probe was supported between two pieces of aluminum condenser tubing with plastic adapters. A-C power was supplied to the ribbons after stabilizing by a Raytheon voltage stabilizer and converted to D-C power by a Selenium rectifier. A wiring diagram of power supply is shown in Figure 5. The current flowing in the circuit was measured by a Weston ammeter. The emf developed due to temperature difference between the 7 hot junctions and one hot junction in the flowing air and a reference cold junction were measured with a Leeds and Northrup precision potentiometer. Values were read to 0.001 millivolts. The thermocouple connections and the wiring diagram are shown in Figure 6.

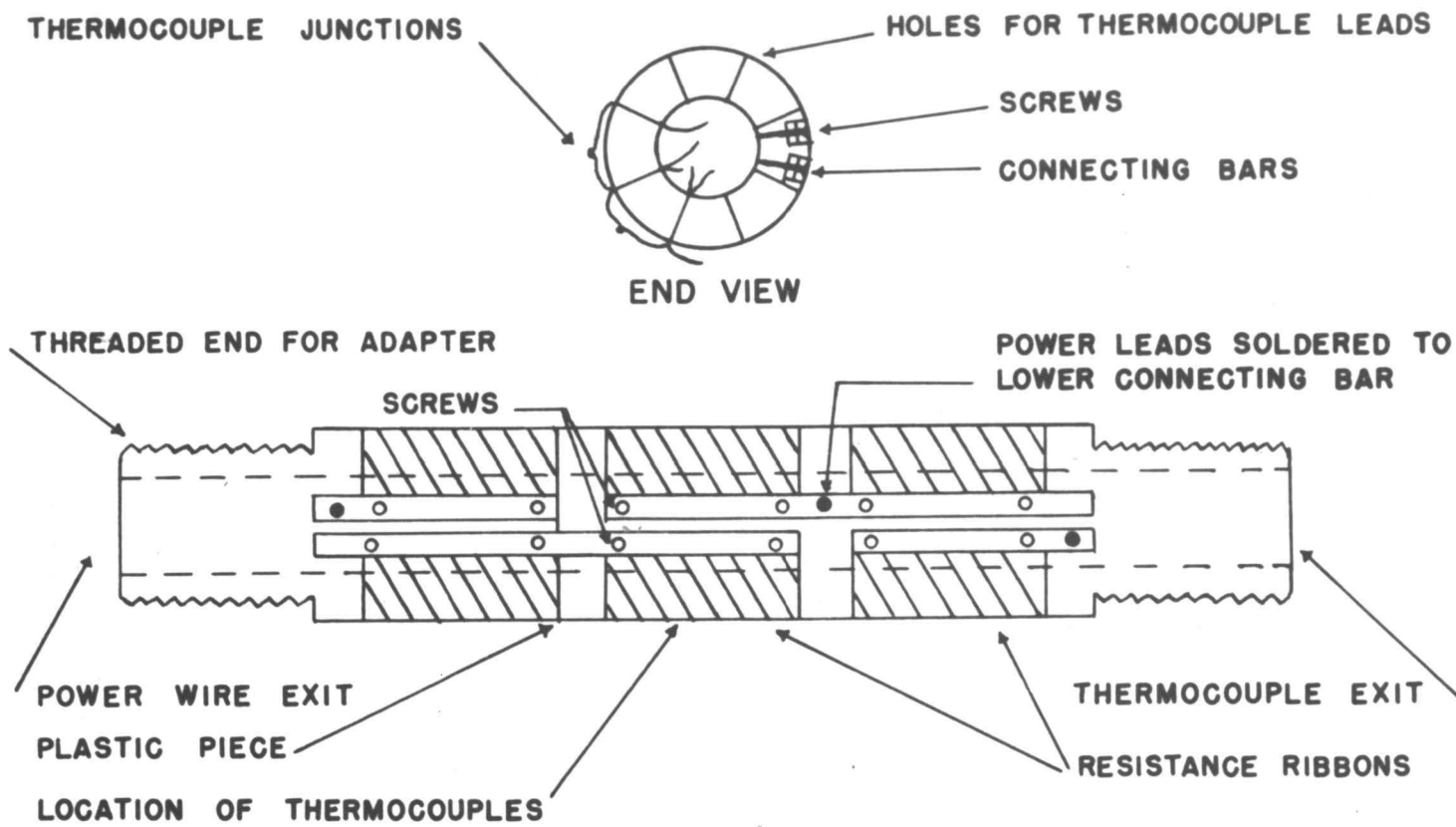


FIGURE 4 DRAWING OF ASSEMBLED SENSING PROBE

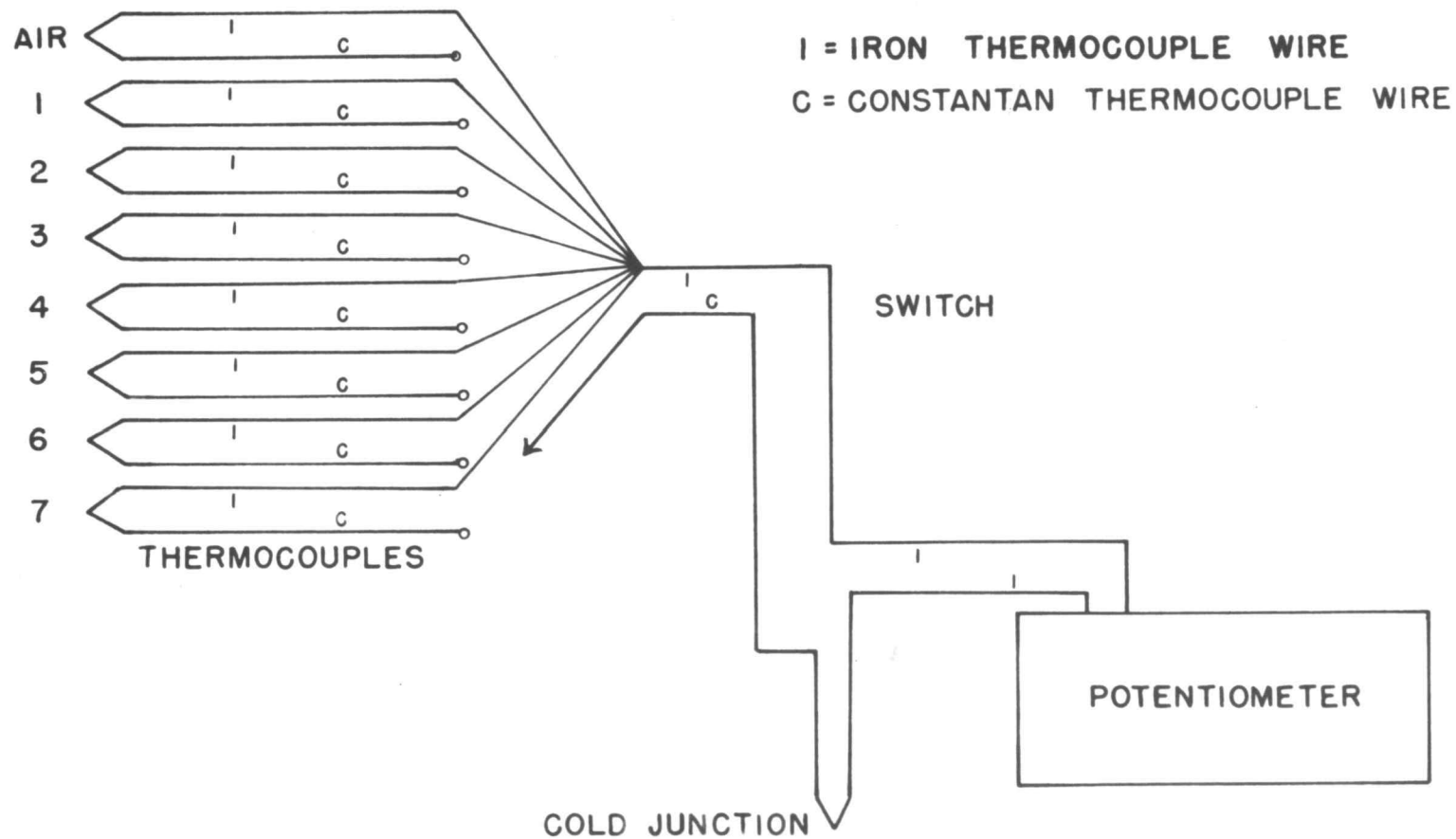


DIAGRAM OF EMF METERING SYSTEM  
FIGURE 5

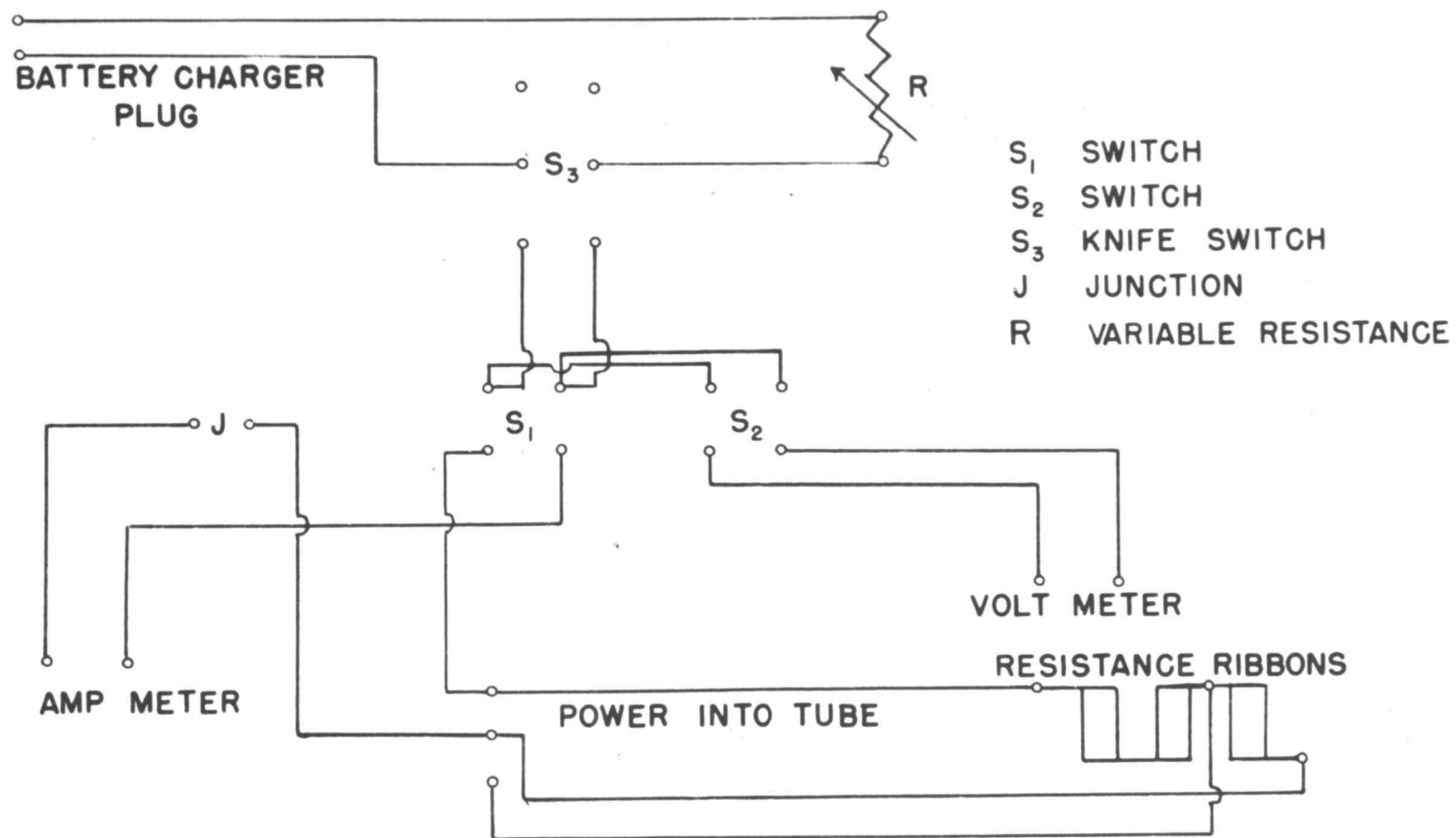


FIGURE 6

WIRING DIAGRAM FOR POWER SYSTEM

### 3. The Air Source and Cooling System

A Roots-type blower rated at 280 cubic feet per minute at  $3\frac{1}{2}$  psig was used to pump the air which was used as the shell-side fluid. The air flow system is shown in Figure 7. Air from the blower passes through two coolers, a calming section on to an orifice meter and into the exchanger. It is discharged through a muffler into the atmosphere. Valves are provided to control and bypass the air flow in the exchanger. Two manometers for the orifice and another for measuring the pressure drop across the exchanger were used. The two manometers for the orifice were connected in parallel and had liquids of densities 0.830 and 2.948 to facilitate more accuracy in measuring low and high rates of flow respectively. Two pressure gauges, one before the orifice and another before the exchanger were used to permit calculation of the flow rate.

More constructional details of the apparatus are given by Ambrose (1,p.32-56).

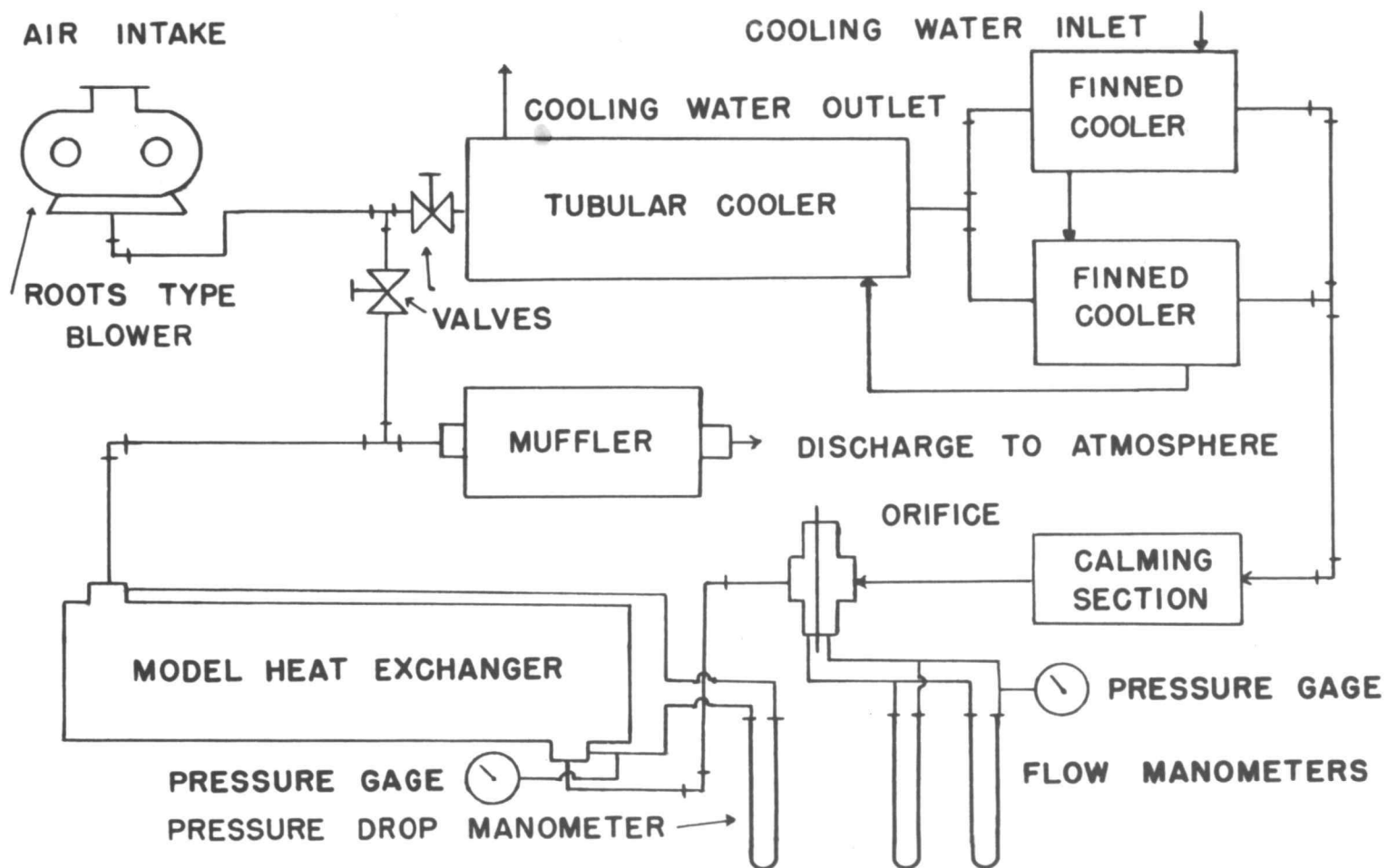


**FIGURE 7 AIR FLOW SYSTEM**

## SECTION IV

### EXPERIMENTAL PROGRAM

An understanding of the dynamics of the fluid flow and the heat transfer being the chief aim of the investigation, it was decided to restrict the study to the space between the two central baffles. Also only one tube spacing of 1 1/4-inch triangular pitch for a fourteen tube bundle was studied. This area will be hereafter referred to as the central chamber.

#### 1. Investigation Positions

To obtain a detailed picture, local heat transfer coefficients on each tube of the fourteen tube bundle were determined at three quarters of an inch intervals for the entire central chamber for two baffle spacings of 6.43 and 4.09 inches and three flow rates of 60, 90, and 120 cubic feet per minute. The intervals were smaller in the vicinity of baffles since a sudden drop of heat transfer rate was expected. The baffle spacings and the positions investigated are shown in Table 2. Also Figures 12, 13, 14, 15, 16, and 17 show the positions investigated and the local heat transfer data at those cross sections.

## 2. Baffle Spacings

Two baffle arrangements with six and ten baffles were deemed sufficient to confirm the findings of Ambrose (1, p. 114) as to the effect of baffle spacing. To facilitate a closer examination without involving too much of work, the short spacings of 6.43 and 4.09 inches were chosen. Details of these arrangements are shown in Table 2.



## Baffle Arrangement in Model-Heat Exchanger

Baffle Spacing

Number of Tubes	Number of Baffles	Baffle Spacing inches	Distance Between Baffles - inches
14	6	6.43	6.30
14	10	4.09	3.97

Investigation Positions

Investigation Position Number	Distance Measured From The Upstream End--inches	
	6 Baffles	10 Baffles
1	19.29	20.45
2	19.50	21.00
3	20.25	21.75
4	21.00	22.50
5	21.75	23.25
6	22.50	24.00
7	23.25	24.55
8	24.00	
9	24.75	
10	25.50	
11	25.72	

To get a sufficiently wide range of Reynolds numbers three flow rates were selected: 60 cfm. 90 cfm. and 120 cfm. Sixty cubic feet per minute was found to be the minimum rate of flow to assure sufficient turbulence and to provide a comparison between the measurements made by Ambrose ( 1, p. 66), since a majority of his data were for a flow rate of sixty cubic feet per minute. Flow rate higher than 120 cubic feet per minute were found to result in excessive leakage at the joints in the exchanger and also in the air cooling coils which could go unnoticed resulting in erroneous results. This range of flow rates provided a Reynolds number range from 10,000 to 26,000.

#### 4. Thermocouple and Tube Numbering System

The method of thermocouple numbering was the same as that of Ambrose (1, p. 59), Tube numbering and thermocouple numbering arrangements are shown in Figure 11. The thermocouples are numbered anticlockwise from an arbitrary line on the air exit side of the exchanger. Positions on the tubes were indicated by the angle measured from a point on the tube on the exit side of the exchanger. The tube diameter drawn along this point is parrallel to the plane passing through the axis of the entrance and the exit of the exchanger. The first

junction is located at  $22\frac{1}{2}^{\circ}$  and succeeding junctions at intervals of  $45^{\circ}$ . The seventh junction is located at  $292\frac{1}{2}^{\circ}$ . Tube numbering is different from that of Ambrose (1, p. 59).

## SECTION V

## EXPERIMENTAL PROCEDURE

The procedures adopted in the present study and by Ambrose (1, p. 67) were the same. The steps performed in operating the equipment and recording the data are listed below in order.

A. Several preliminary preparations were made before starting the equipment.

1. Ice was placed in the thermos bottle and the cold junction of the thermocouple was well submerged in it.
2. The potentiometer was balanced against the internal standard cell.
3. The sensing probe was placed in the first tube location and the first position to be studied. The position of the probe was adjusted by noting the figures marked along a horizontal line marked on the probe.

For example the first position in the 6 baffle case was 19.29 inches from the upstream end. The mark on the probe read 19.29 inches from the upstream end. The mark on the probe read 19.29 0.75 inches. Another check was to see whether the center of the central ribbon was

on the baffle or not. The same test was applied in the last investigation also.

4. The tube position, number of baffles, flow orifice size and the barometric pressure were recorded.
5. Temperature of the air was measured by a thermometer and the measurements of the millivolt readings of the potentiometer checked.
6. The water was opened allowing cooling water to flow through the air coolers.
7. The bypass valve was completely opened and the heat exchanger valve closed.

B. After all the preliminary operations the following were carried out:

1. The blower was started and the rate of flow of air into the exchanger regulated by the control valves.
2. The electrical switches were all turned on.
3. The ribbon temperature was allowed to come to equilibrium and the emf across each thermocouple was measured with the potentiometer. Generally it took between five and ten minutes to reach equilibrium. The millivolt readings of the seven probe thermocouples and one air

thermocouple were read and recorded. The measurements were checked again after two minutes. If they did not change they were finalised. If they changed the measurements were started over again.

4. The ammeter was read and recorded.
5. The pressure drop and flow manometers were read and recorded.
6. The pressures at the upstream side of the orifice and the heat exchanger were read and recorded.

C. At the completion of the operations in part B, the position of the sensing probe was changed and the procedure from B3 to B6 repeated for this new position. The adjustment of the probe position was done as described under A-3. Eleven positions in the case of 6 baffles and 7 positions in the case of 10 baffles were studied.

- D. When all the positions were completed,
1. The power supply was shut off,
  2. The air blower was turned off and
  3. The orifice was changed for the next desired flow rate. For the three flow rates of sixty, ninety, and one hundred and twenty cubic feet

per minute, orifices of size 1 inch, 1.25 inches and 1.5 inches respectively were used.

The same procedure from B-1 to D-3 was repeated for all the three flow rates.

## SECTION VI

## CALCULATION OF DATA

A general expression for calculating the heat transfer coefficient from measured temperatures is developed by making an energy balance around a differential length of resistance ribbon shown in Figure 8. The energy balance is as follows:

(heat conducted in) + (heat generated) = (heat convected to fluid) + (heat radiated to surroundings) + (heat conducted into plastic cylinder).

Writing this in symbol form and simplifying gives

$$h = \frac{\frac{i^2 R}{w} + \frac{kZ}{Wr^2} + \frac{d^2 t}{d\theta^2} - \frac{\text{rad}}{A} - \frac{\text{cond}}{A}}{t - t_a}$$

The radiation and the conduction terms are very small compared to the other terms in most of the cases and could be neglected without introducing any serious error. These assumptions are in agreement with other investigators who have used this method.

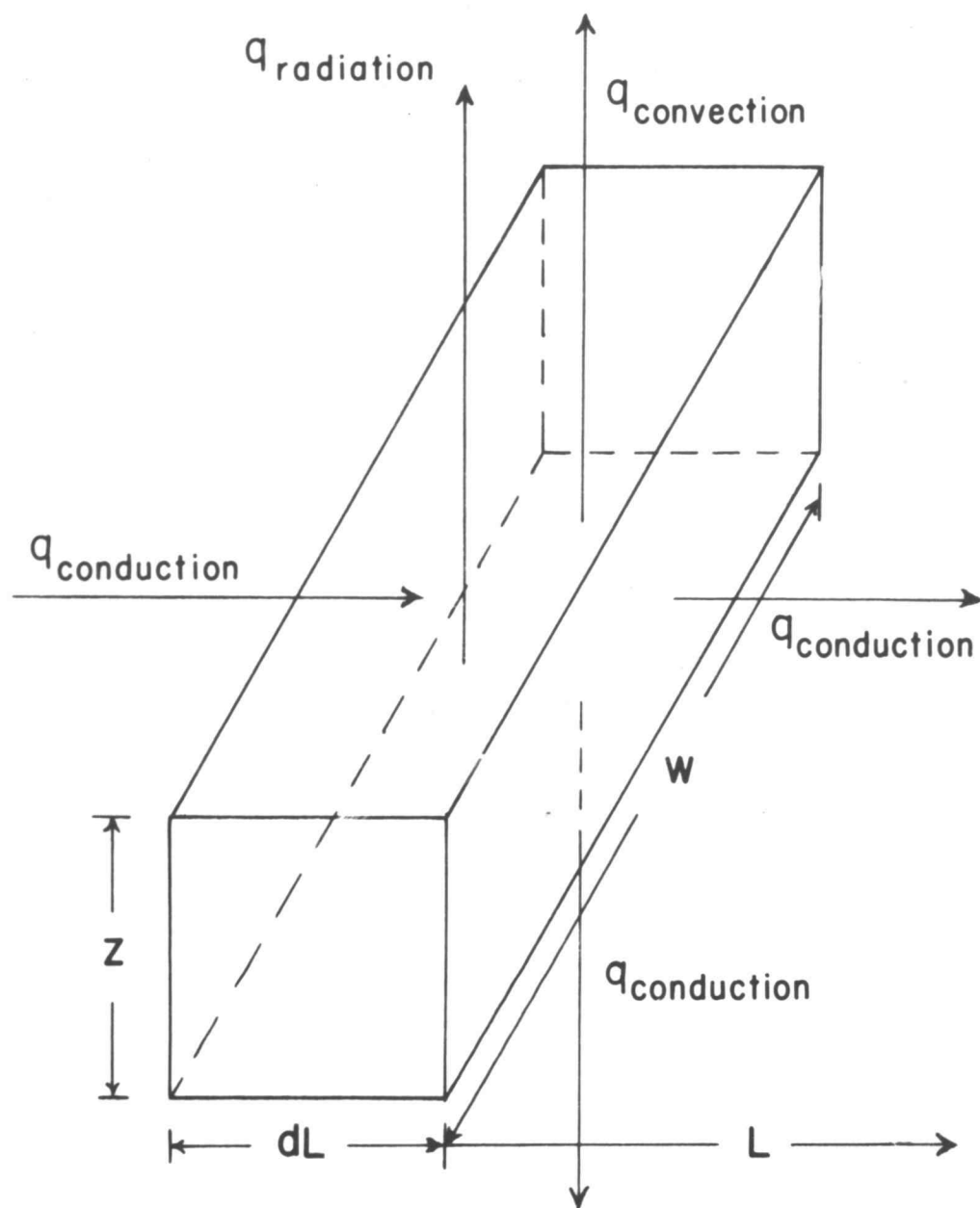
Substituting the numerical constants, the equation becomes

$$h = \frac{11.10 i^2 + 2404 \frac{d^2 t}{d A^2}}{t - t_a}$$

This equation was used to calculate the local heat transfer coefficients from observed data. The second



derivative of the temperature with respect to angle was evaluated using a Milne three point method (24). The actual calculation of the local heat transfer coefficients was performed on an Alwac III E digital computer. The program used is included in the appendix. An average heat transfer coefficient was evaluated at each position from the arithmetic average of the local coefficients around the circumference of the tube. A Nusselt number for each position was calculated using this average heat transfer coefficient, the tube diameter and the thermal conductivity of air at the temperature existing in the heat exchanger. The methods of calculation of flow of air and calculation of the average values of the Nusselt numbers were the same as Ambrose (1, p. 79-88). The equations used are furnished in the appendix. The flow rates were also calculated on the Alwac III E digital computer and the program used is included in the appendix.



DIFFERENTIAL LENGTH OF RESISTANCE RIBBON  
FIGURE 8

## SECTION VII

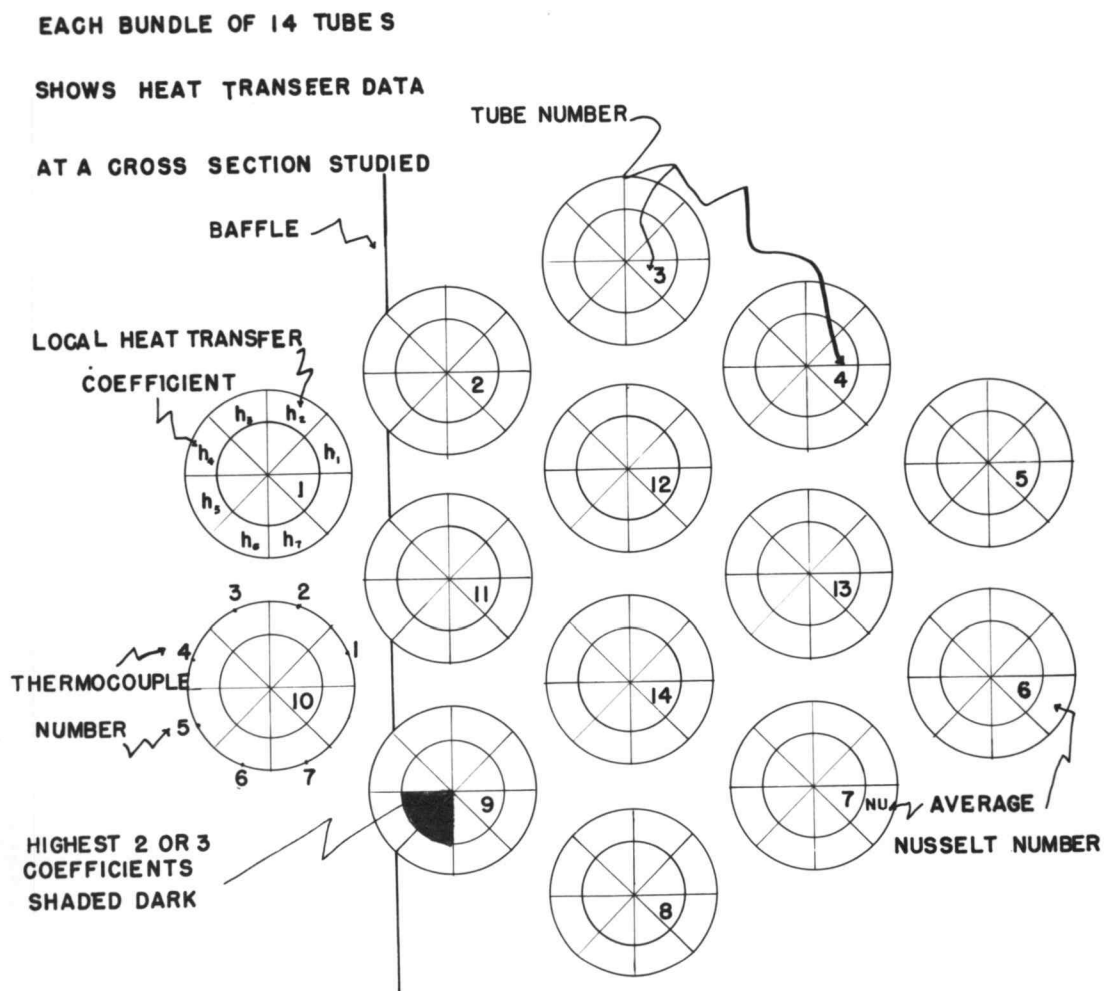
## ANALYSIS OF DATA

1. Presentation of data

The local shell-side heat transfer data are presented in a picture form in Figures 12, 13, 14, 15, 16, 17 and 20. The variation of heat transfer rate along and around each of the 14 tubes in the bundle can be easily seen from these figures. The two or three highest values of these local coefficient are shaded black. This helps to indicate more clearly what is happening in the exchanger. Examination of these figures permits the sketching of an approximate flow pattern in the baffle space. A schematic diagram of the flow pattern is shown in Figure 20 which indicates the various zones and from this it can be seen why the heat transfer coefficients vary as they do. Consequently this method of presentation is considered to be a good way to present the data.

2. Correlation of Data

Properly weighted overall shell-side overall heat transfer rates for the model heat exchanger were calculated and compared with published values. The correlations of Ambrose (1, p. 91) and Williams and Katz (35) were



GRAPHICAL PRESENTATION SYSTEM OF HEAT TRANSFER DATA  
FIGURE 11

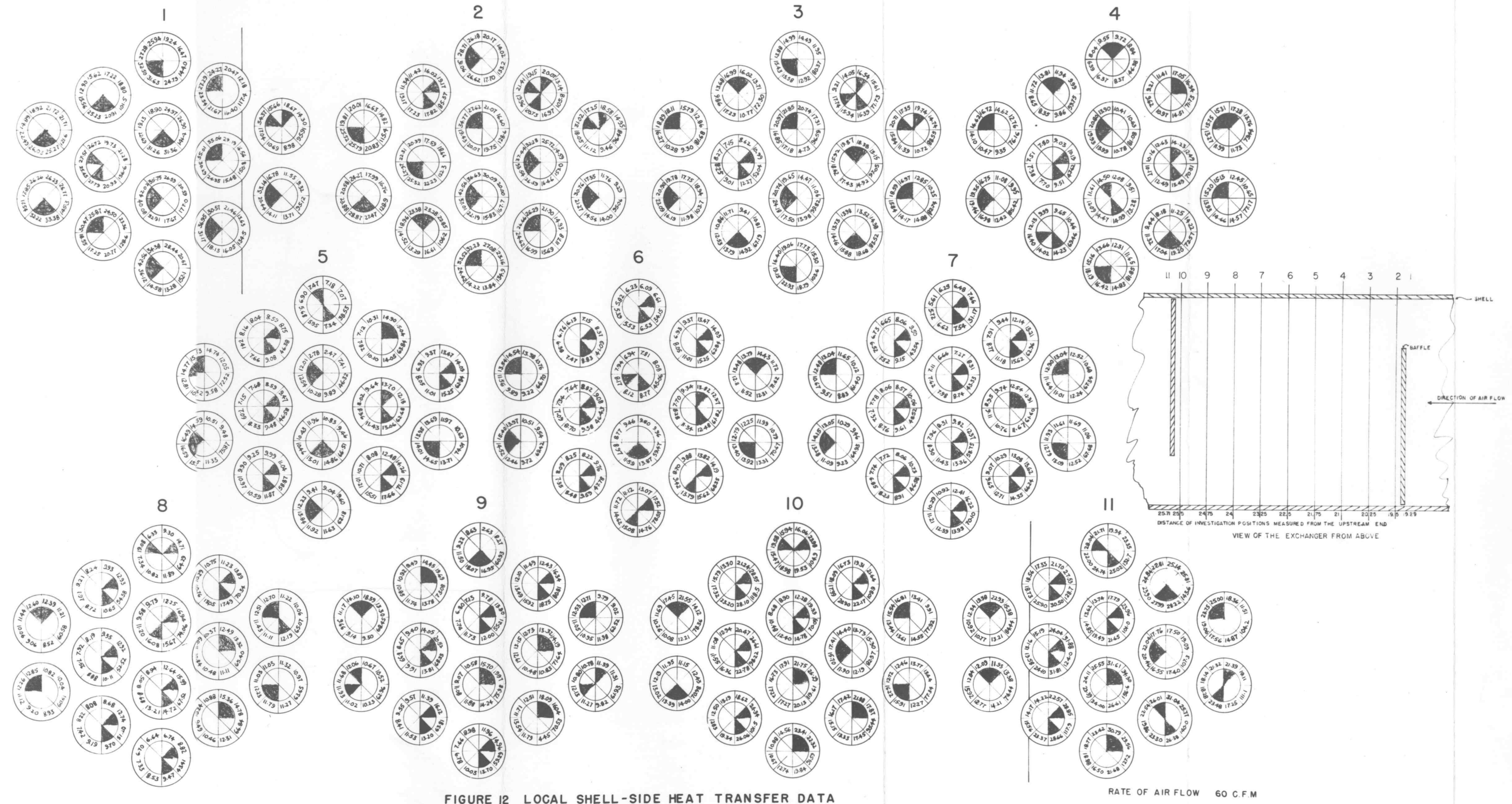


FIGURE 12 LOCAL SHELL-SIDE HEAT TRANSFER DATA  
IN A BAFFLED TUBULAR HEAT EXCHANGER



RATE OF AIR FLOW 90 C.F.M

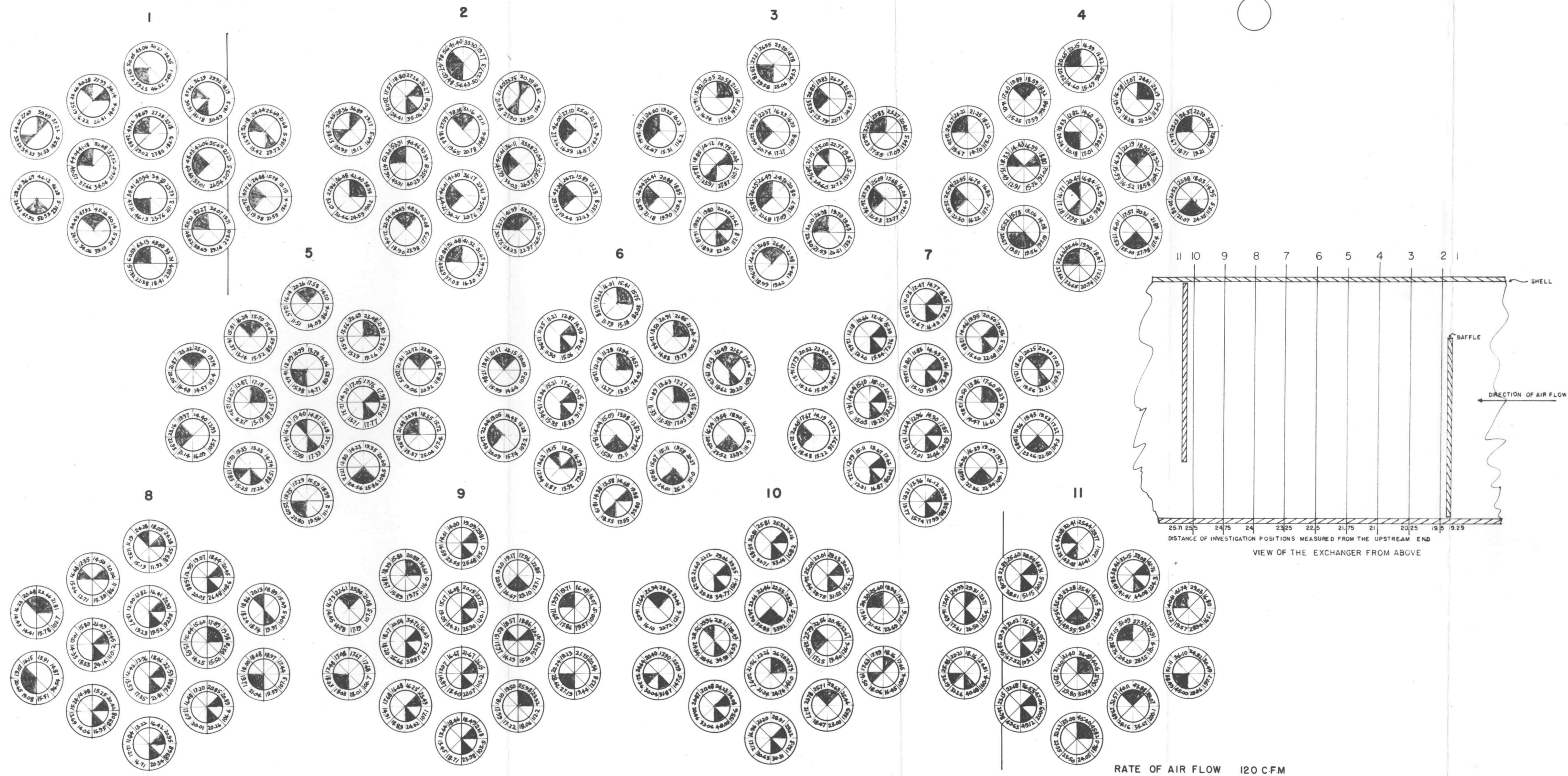


FIGURE 14 LOCAL SHELL-SIDE HEAT TRANSFER DATA  
IN A BAFFLED TUBULAR HEAT EXCHANGER

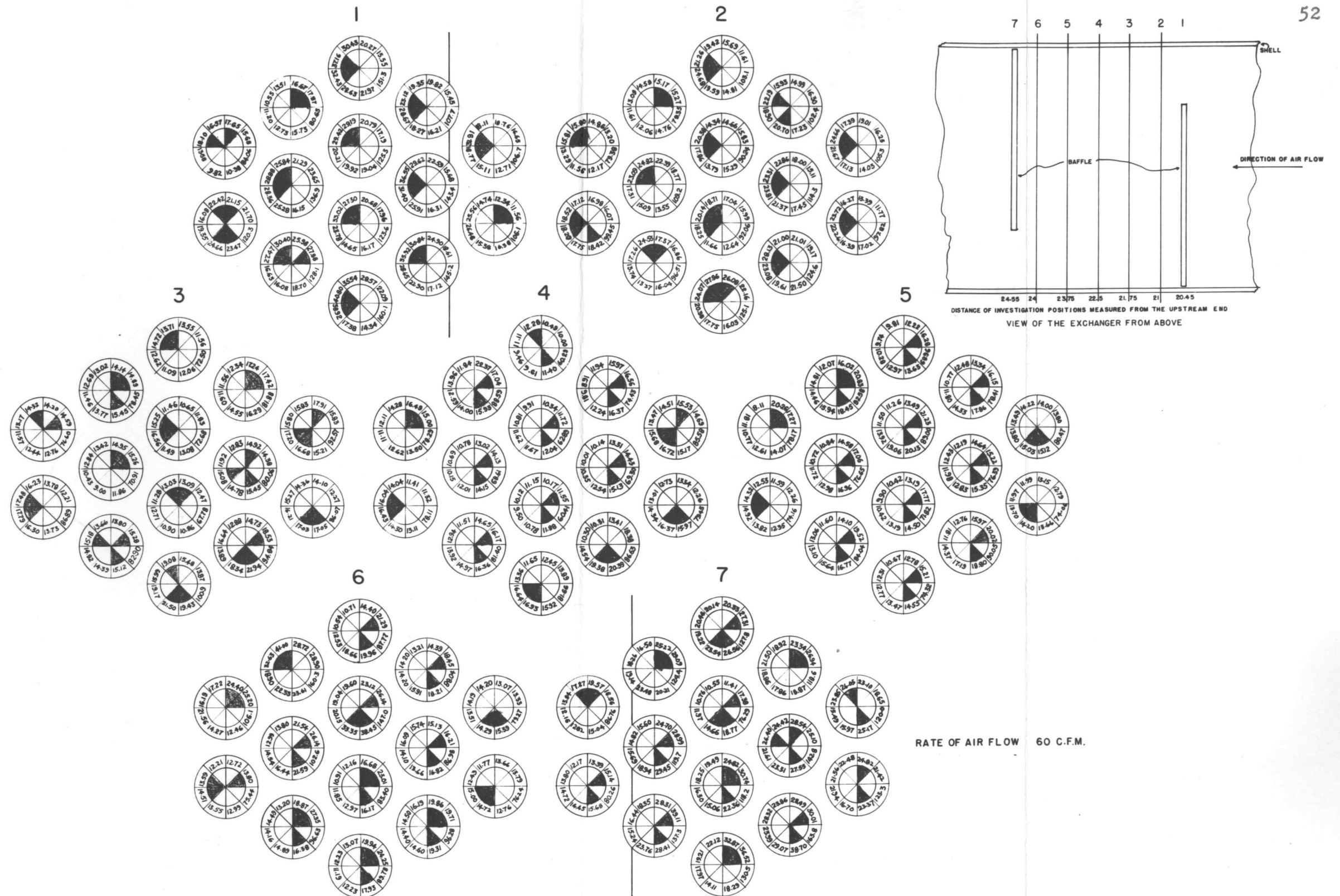


FIGURE 15 LOCAL SHELL-SIDE HEAT TRANSFER DATA  
IN A BAFFLED TUBULAR HEAT EXCHANGER



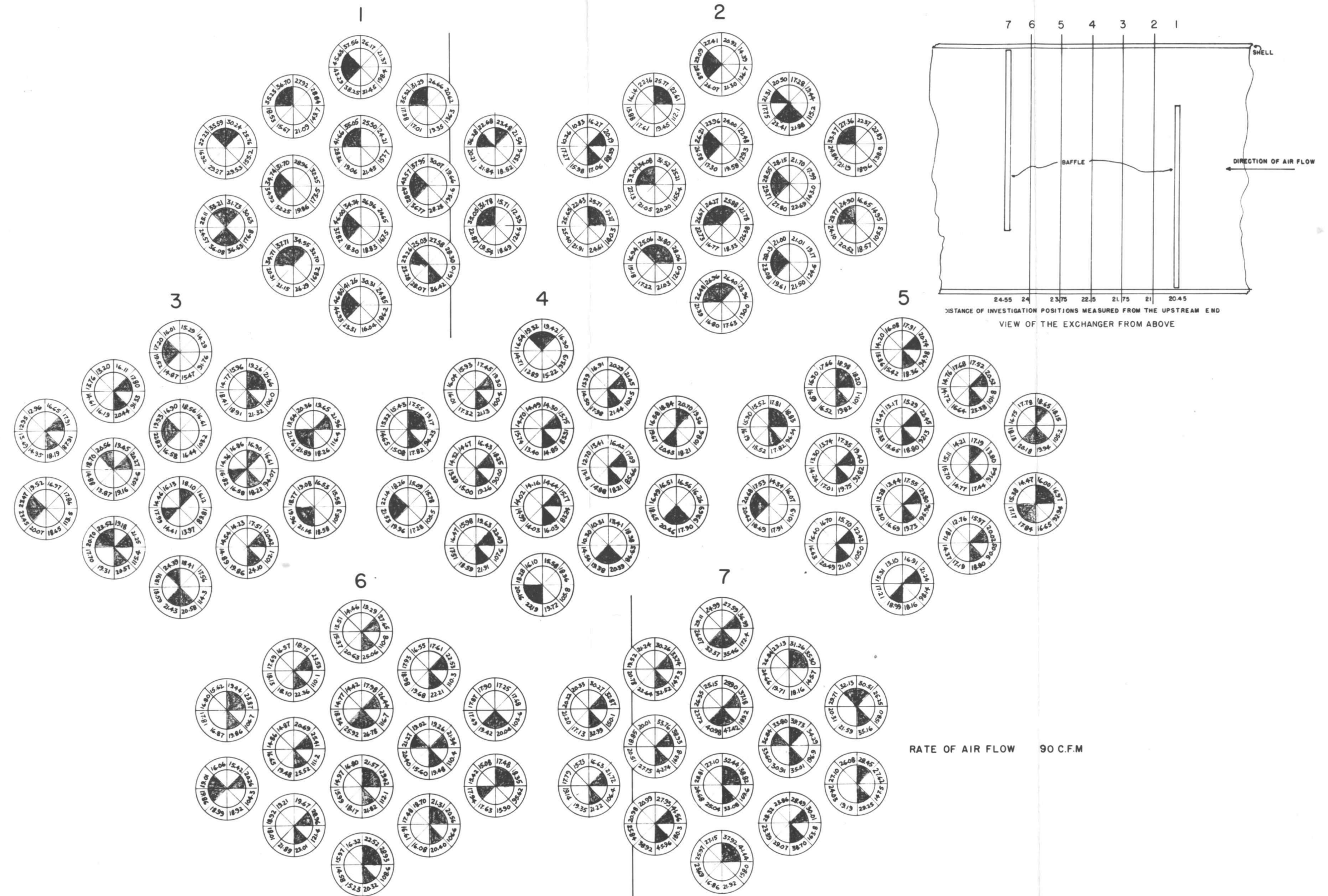


FIGURE 16 LOCAL SHELL-SIDE HEAT TRANSFER DATA  
IN A BAFFLED TUBULAR HEAT EXCHANGER

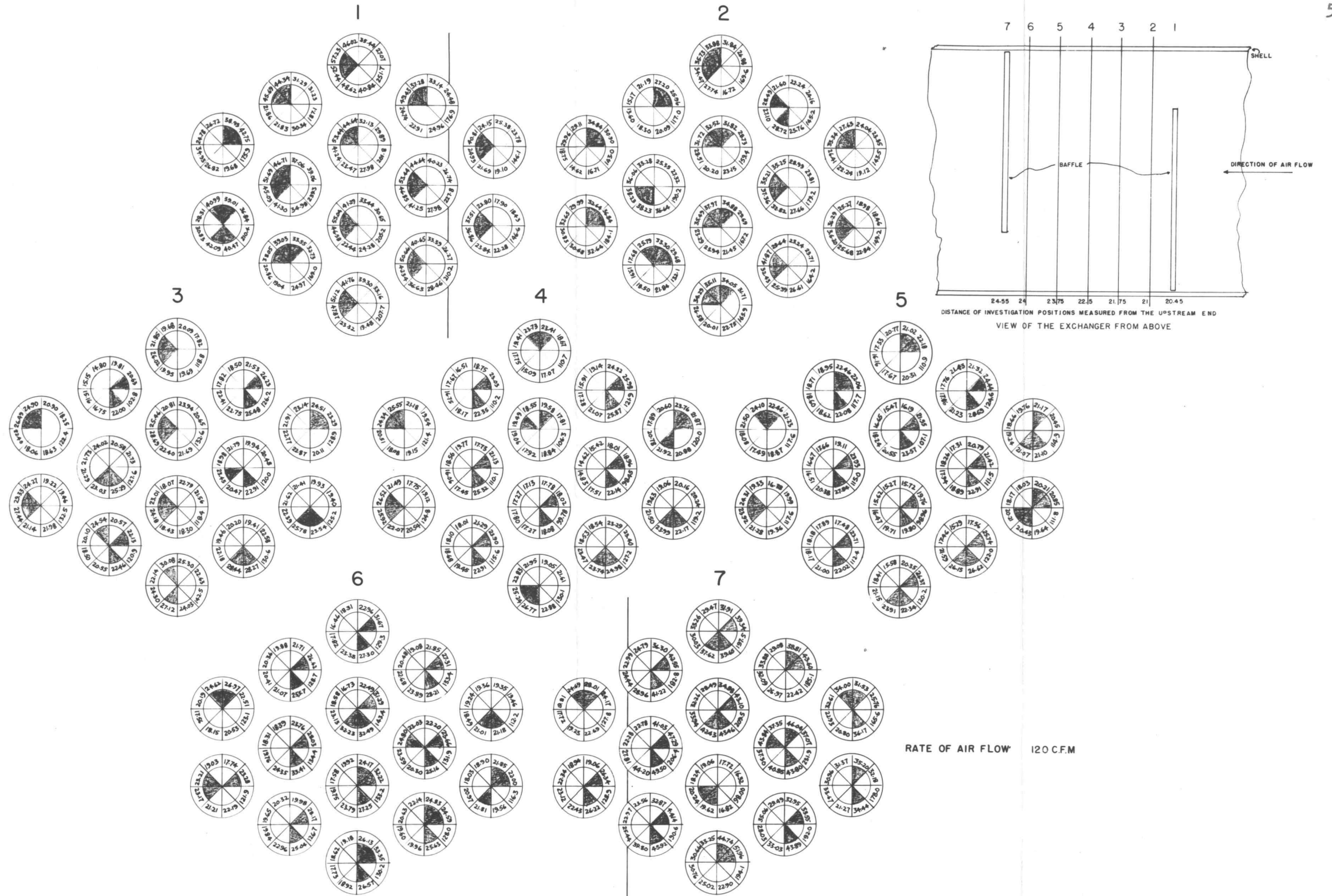


FIGURE 17 LOCAL SHELL-SIDE HEAT TRANSFER DATA  
IN A BAFFLED TUBULAR HEAT EXCHANGER

chosen for comparison since their investigations were carried out under similar conditions and the correlations were also similar.

The correlation of the present work compares very favorably with the work of Williams and Katz (35) and Ambrose (1).

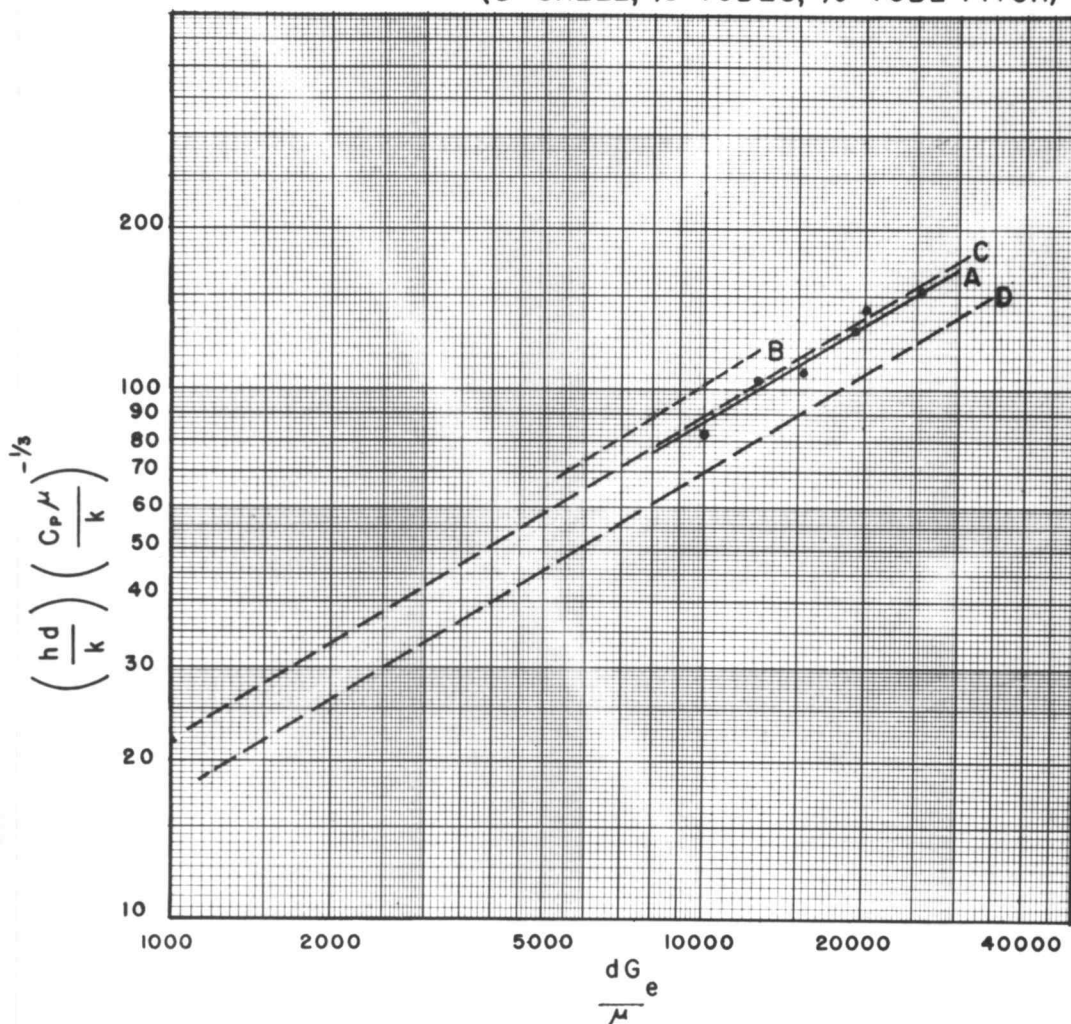
The dimensionless term  $\left(\frac{hd}{k}\right)\left(\frac{c_p \mu}{k}\right)^{-1/3}$  was calculated from the average Nusselt number and the Prandtl number of air which was taken as 0.7 in all cases. The results are shown in Table 3 and Figure 9. This term was plotted versus the weighted Reynolds number. A straight line of slope 0.6 was obtained. On the same plot, the correlations of Ambrose (1, p. 92) and Williams and Katz (35) are shown for comparison. The straight line B of Ambrose (1) is somewhat high but line C of Williams and Katz (35) is very close to the data. Ambrose (1) used the 1 inch tubes and the 1 1/4 inch tube pitch as was done in the present investigation but this data included the cases of 2 and 4 baffles in addition to the 6 and 10 baffles investigated in the present work.

Ambrose's results are somewhat higher than the present ones. The reason for this can be found in the method of determining average Nusselt numbers along the tube. Ambrose investigated 3 to 4 cross-sections in each baffle space and in determining the average Nusselt

number he assumed linear variation of the heat transfer coefficient between the points studied. In the present work 11 cross-sections in a baffle space were studied. The curves shown in Figure 18 and 19 show in great detail the variation of the heat transfer coefficient along the tube. Integration of these curves gives an average coefficient for the tubes. The resulting coefficient is more accurate than those obtained by Ambrose and also somewhat smaller since the curves obtained by Ambrose are based on only 3 or 4 values in the baffle space.

Lines C and D in Figure 9 are those of Williams and Katz (35). Line C is for a segmental baffled tubular heat exchanger with a 6-inch shell diameter,  $5/8$  - inch tubes and  $3/4$  - inch tube pitch, and D line is for a 8 - inch shell diameter,  $1/2$ -inch tubes and  $5/8$  - inch tube pitch. Line C is associated with a tube size to tube pitch ratio of 0.834 and line D is associated with a tube size to tube pitch ratio of 0.8. The present correlation with a tube size to tube pitch ratio of 0.8 is closer to line C than line D. This is expected for two reasons, the first is that the heat transfer rate should increase with the increase in tube size or the clearance when the ratio of tube size to tube pitch is held constant. The second is the fact that there were

- A GURUSHANKARIAH (6" SHELL, 1" TUBES, 1 1/4" TUBE PITCH)  
 B AMBROSE - do -  
 C WILLIAMS AND KATZ (6" SHELL, 3/8" TUBES, 3/4" TUBE PITCH)  
 D WILLIAMS AND KATZ (8" SHELL, 1/2" TUBES, 3/8" TUBE PITCH)



CORRELATION OF SHELL-SIDE HEAT TRANSFER DATA

FIGURE 9

no clearances between baffle holes and tubes in the case of line C. This is one of the conclusions of Ambrose (1, p. 117). The reason for the line A being slightly lower than line C may be explained by the lower tube size to tube pitch ratio of 0.8 for A as against 0.834 for C. However, all the straight lines have the same slope of 0.6 so the results shown in Figure 9 indicate good agreement of the present work with those of other investigators.

### 3. Comparison with Measurements of Ambrose (1)

Since measurements were made with the same apparatus, there were three common cross-sections investigated by both Ambrose and the author. These data were compared as a further check on the present work. Average Nusselt numbers were plotted versus the tube positions in Figure 10 - A, B and C. The cross-sections considered are at the center of the central chamber for both the 6 baffle case and the 10 baffle case and on the baffle on the upstream side of the central chamber. They appear to be in good agreement. Two noticeable changes in C are tube number 2 and 9 which have lower average Nusselt number. This can be explained by the fact that they are right in the baffle cut where the turning of the flow occurs. Curve B is in good agreement. Curve A has a small



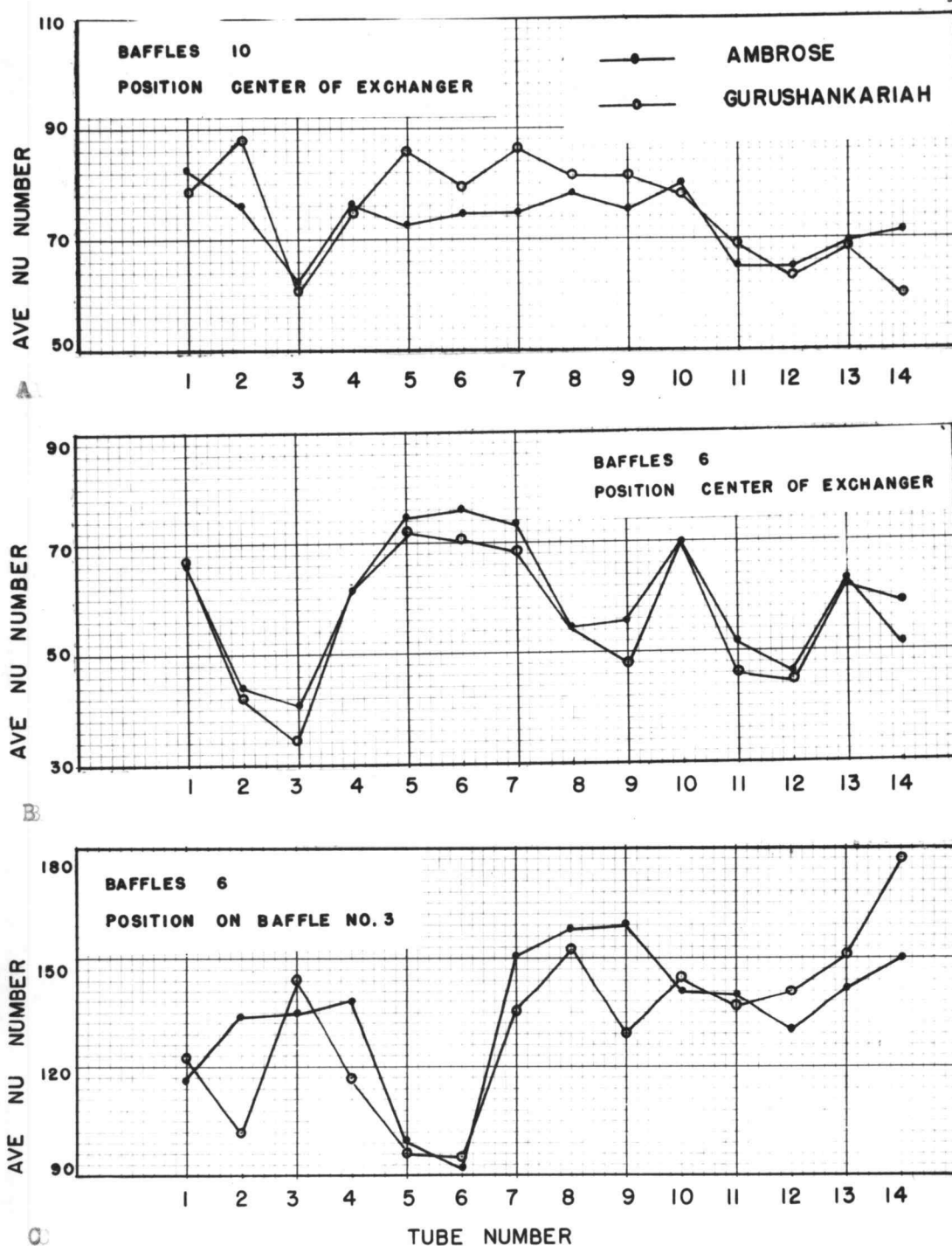


**FIGURE 10 COMPARISON OF AVERAGE NUSSELT NUMBERS  
WITH MEASUREMENTS MADE BY AMBROSE**

divergence from tube number 5 to 9. However, fair agreement in the general tendency is observed in all these three cases. This comparison indicates a fair reproduction of the results obtained by Ambrose (1) and support the reliability of the present results.

### 3. Discussion of Data

#### (a) Effect of Baffle Spacing

The addition of baffles decreases the baffle spacing and increases the number of passes and the local mass velocities across the tube bundle. Consequently the heat transfer coefficient is increased. It also increases the pressure drop. This effect is shown by Ambrose (1, p. 114). Increases of heat transfer coefficient as high as 160 per cent over the unbaffled case and 23 per cent over the 6 baffle case were noted in his work in the case of 10 baffles. In the present work the same effect is noticed also. Table 6 shows the variation of average Nusselt number for the two baffle spacings of 6.43 inches and 4.1 inches. Per cent increase of average Nusselt number in the case of 4.1 inches baffle spacing over the 6.43 inches baffle spacing is as high as 25.5 per cent at a flow rate of 60 cubic feet per minute. No comparison to the unbaffled case was possible since no data were taken for that case. The baffle spacing of 4.1 inches appears



to be the minimum that can be adopted since a further decrease might reduce the turbulence in the baffle space to the point where a reduction of heat transfer rate will occur. This effect can be noticed in Figures 12, 13, 14, 15, 16, 17 and 20.

There is definitely less turbulence in the 10 baffle case than in the 6 baffle. Increase of the number of baffles also increases the pressure drop.

#### (b) Effect of Flow Rate

An increase in the flow rate increases the heat transfer rate. This is noted in both the 6 baffle case and the 10 baffle case. Considering the per cent increase in Nusselt number for a flow rate of 120 cubic feet per minute over the Nusselt number for a flow rate of 60 cubic feet per minute, there is an increase as high as 73.35 per cent in the 6 baffle case and an increase as high as 48.16 per cent in the 10 baffle case.

The lower increase in the 10 baffle case was probably due to lesser scope for increased turbulence in the restricted space. The results are shown in Table 6. At higher flow rates there was more leakage through the baffle holes which brought about more turbulence in the eddy zone. This effect was more pronounced for the large baffle spacing. This effect can be observed in Figure 20.

The effect of flow rate in the different flow zones is discussed under a separate heading.

(c) The Effect of the Clearance Between the Tube and Baffle Holes

It appears that a small clearance between the tube and baffle holes causes an increase in the heat transfer coefficient. This is evident from the high Nusselt numbers at the baffle and very close to it. The average values of Nusselt number with and without including these high values are shown in Table 7. The percentage increase of the high values over the low values indicates to some extent the effect of the clearance between the tube and the baffle hole. It is interesting to note that the effect is more or less the same for all the flow rates but varies with the baffle spacing. The difference is around 15 per cent in the case of 10 baffles and 22 per cent in the case of 6 baffles. The true effect of tube to baffle clearance can only be determined by comparison with an exchanger in which there are no clearances.

(d) Flow Pattern

As indicated earlier the flow pattern on the shell-side of a baffled heat exchanger is very complicated. It is much more complex where there are many structural

clearances like the clearance between the baffle and the shell baffle holes and the tubes which cause leakage of the flowing fluid and disturb the flow pattern.

#### 1. Clearance Between Tube and Baffle Hole

As indicated earlier the leakage flow between the tube and the hole increases the heat transfer coefficient at the baffle and in its vicinity. It also appears to affect the flow pattern in the eddy zone. The direction of maximum local heat transfer coefficients indicate to some extent the direction of flow since the maximum values occur at the leading edge. These indicate in Figure 20 that there are either two different turbulent eddies in the eddy zone with eddies rotating about the axis of the tube or there is a strong effect of the tube and baffle hole leakage resulting in high heat transfer rates.

It is believed that the high coefficients are due to the eddies rotating along the tube axis because the directions of approach of flow to two adjacent rows of tubes are symmetrical and opposite to each other. This happens for two sets of rows. If this effect was due to the leakage flow it should have been uniform around each tube which is not the case. The leakage has at least an indirect effect in causing these two turbulent eddies in the eddy zone.

## 2. Flow Zones

From an observation of Figure 20, the space between two baffles can be divided roughly into three zones. These are longitudinal flow, cross-flow, and eddy flow zones. The longitudinal flow occurs in the baffle windows. The cross-flow and the eddy flow more or less divide the chamber between the baffles into two equal parts. The eddy zone is on the upstream side of the space. The cross-flow forms the bulk of the stream in the baffle space. In the eddy zone the fluid separated from the cross-flow stream goes through the eddies and rejoins the main stream. Flow in the eddy zone is apparently quite turbulent. The flow pattern in the eddy zone seems to be somewhat affected by the leakage through the clearances in the baffle. This effect is more significant in the larger baffle spacing ( six baffles) than for the smaller baffle spacing (ten baffles). The rate of flow of fluid does not seem to affect the flow pattern in the baffle space. The average Nusselt numbers occurring in the various flow zones and the overall values are shown in Table 8. These average values are plotted versus the flow rate in Figure 21. This indicates that the rate of heat transfer increases linearly with the rate of flow in both the longitudinal and cross-flow zones, the lines having approximately the same slope in both the 10 and 6 baffle cases. In the eddy

zone the average Nusselt number increases more rapidly with flow rate than in the other two zones. The curve showing the increase in the eddy zone in the case of 6 baffles has a greater slope than in the case of 10 baffles. Generally the Nusselt numbers in the eddy flow zone are slightly higher than in the other zones. The longitudinal zone comes next in the order of magnitude of the average Nusselt numbers. The slightly greater or equal rate of heat transfer in the eddy zone is contrary to the findings of Cuptha and Katz (16, p. 998-999). In the exchanger studied by these investigators there was no clearance between the baffle and shell or between the baffle hole and tube. This probably accounts for the lower heat transfer coefficients obtained by these workers.

#### (e) Variation of Heat Transfer Rate Along Tubes

Average Nusselt numbers at each investigation position for all the 14 tubes in the tube bundle have been plotted versus the distance of investigation positions measured from the upstream end for the two baffle spacings in Figures 18 and 19. The 14 tubes are divided into 3 groups plotting for easier interpretation. The first group A consists of the four tubes which are located in the baffle windows. The third group C includes all the tubes centrally located and the second group B consists of the

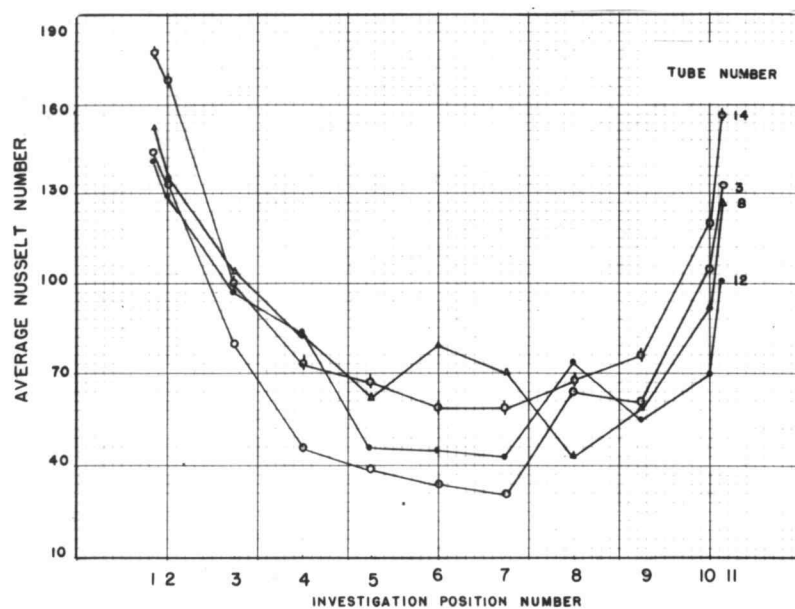
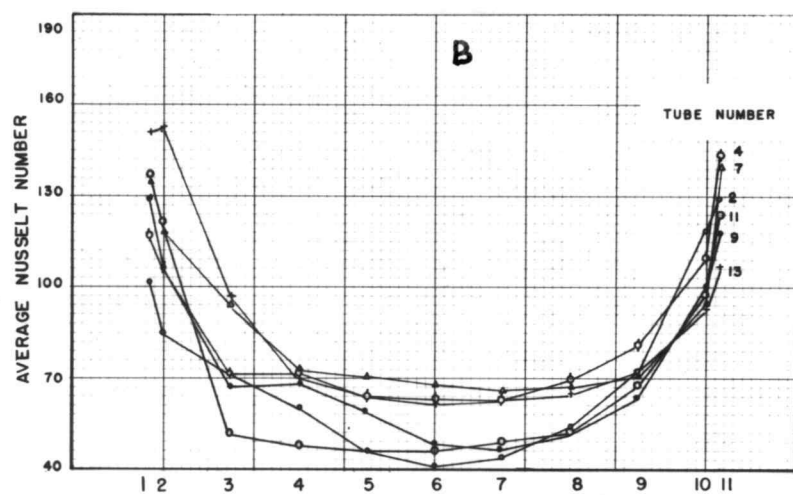
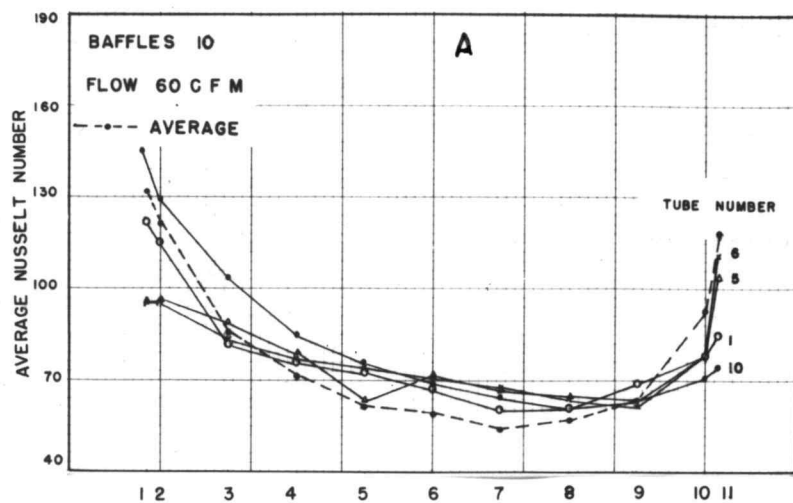


**FIGURE 18 AVERAGE NUSSELT NUMBERS ALONG TUBES**

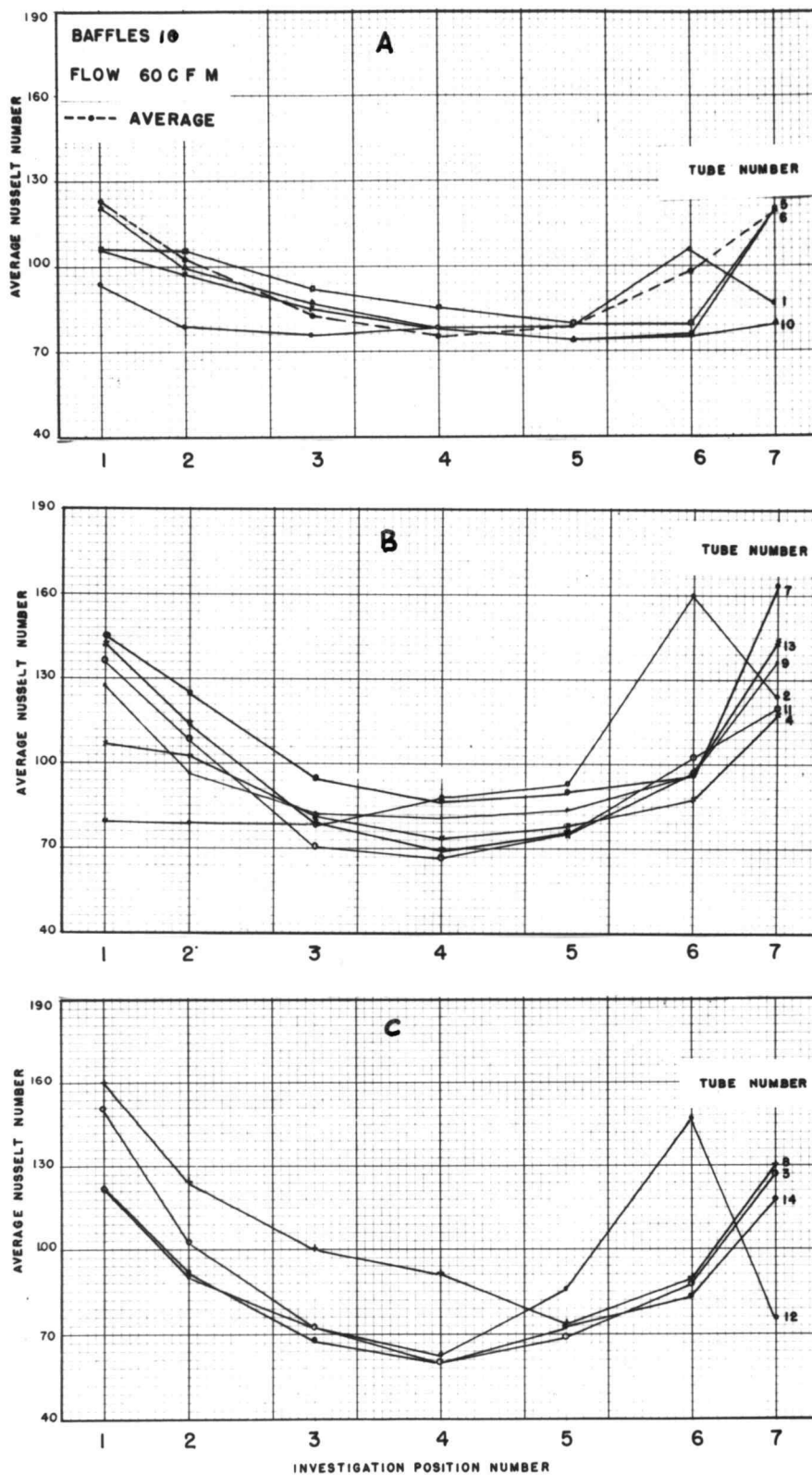


FIGURE 19 AVERAGE NUSSELT NUMBERS ALONG TUBES

remaining tubes.

It is interesting to note that these groups behave more or less similarly and have about the same order of magnitude for the average Nusselt number. All the tubes located in the second group B are practically symmetrical about the center but the first group A and the third group C have higher values on the upstream end and slightly lower values at the downstream end. This is true in both the 6 and 10 baffle cases. The broken curve in Figures 18-A and 19-A shows the average values at each investigation position.

The average curve in Figure 19-A, referring to the 10 baffle case is symmetrical about the center whereas the corresponding curve in Figure 18-A has higher values at the upstream end and lower values at the downstream end. This indicates higher heat transfer coefficients in the eddy zone than in the cross-flow zone in the 6 baffle case. They are equal in the 10 baffle case. The heat transfer rates are maximum at the baffles and a minimum at the center of the space between the baffles. The heat transfer rate decreases by 50 per cent within about an inch from each baffle in both the 6 baffle and 10 baffle case. This indicates the zone affected by the baffle.



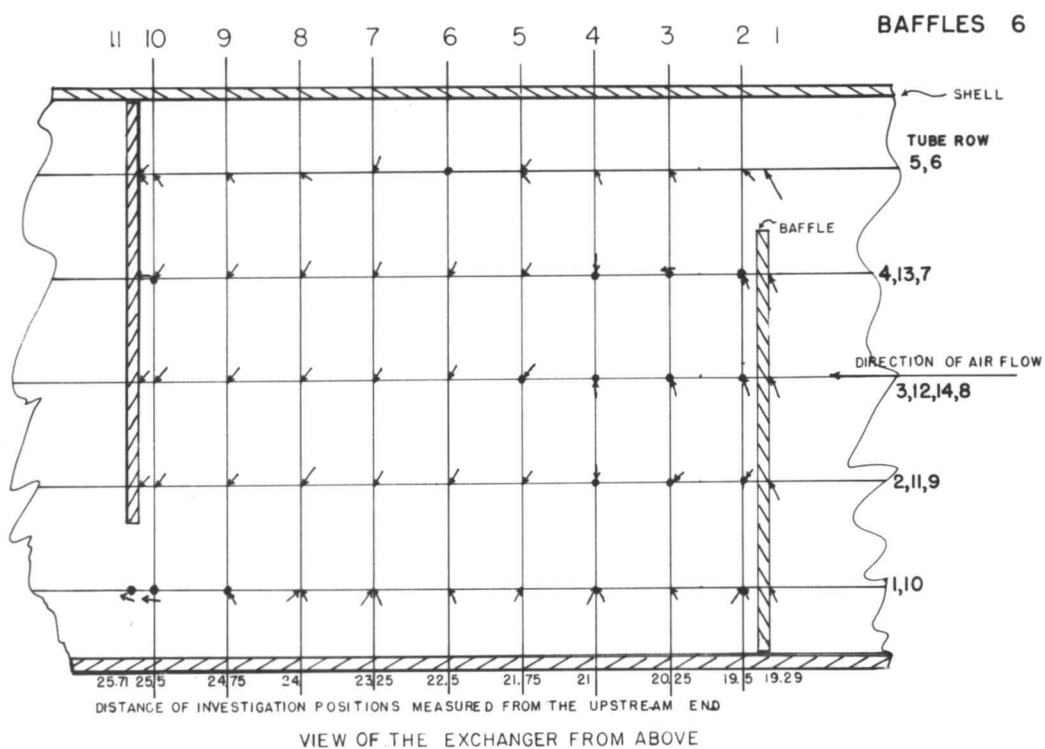
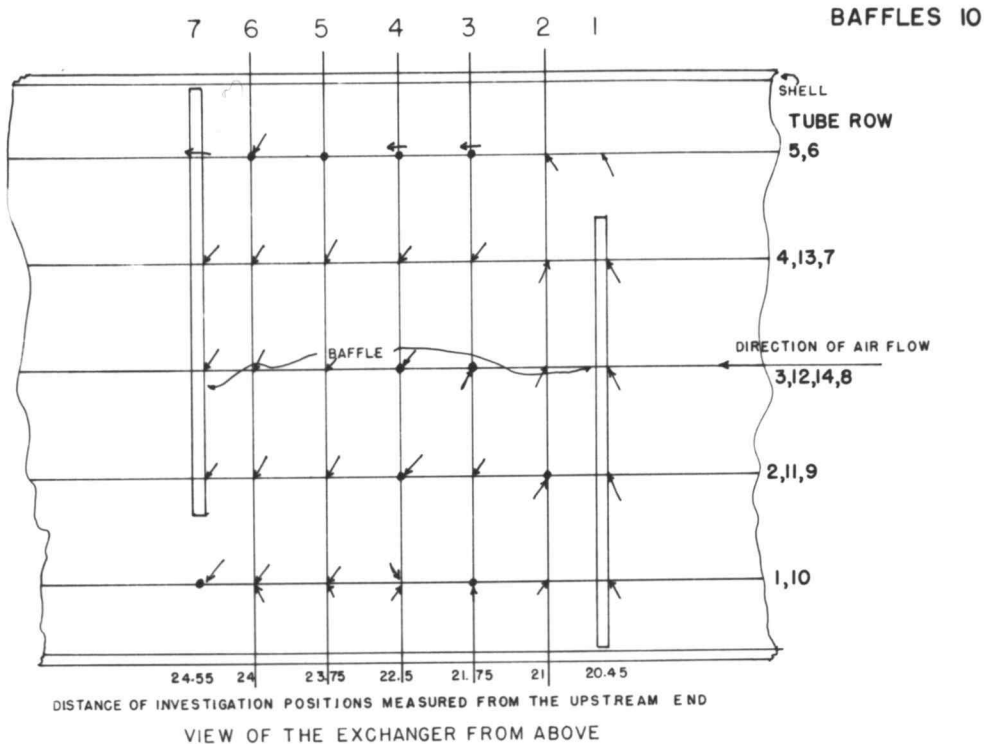


FIGURE 20 SCHEMATIC DIAGRAM OF THE FLOW PATTERN

(f) Variation of Heat Transfer Rate Around Tubes

The variation of the heat transfer rate around the tubes can be easily seen in Figures 12, 13, 14, 15, 16 and 17. The maximum two or three values have been indicated by shading the segment of the circle. These are believed to indicate the direction of fluid flow past the tube since maximum heat transfer coefficients occur at the forward leading edge of bodies immersed in a flowing fluid. This is the basis for the schematic diagram of the flow pattern shown in Figure 20. The variation around a tube is less in the central tubes than in those surrounding them. The maximum heat transfer coefficient around a tube varies from 1.5 to 3.5 times the minimum value.

(g) Experimental Errors and Accuracy Attained

Errors involved in the determination of the local heat transfer coefficients are: errors in reading the emf values for the various thermocouples and the current, the radiation losses from the ribbon and the conduction losses into the probe. A detailed discussion of these errors is made by Ambrose (1, p. 111-113) who also used the same apparatus. The emf of the thermocouples was read to 0.001 millivolts and the current was read to 0.01 amperes

but it was felt that an error of 0.1 °F and 0.02 amperes was possible. The percentage error is 1.65 per cent. Since only one tube out of the tubes in the bundle had heating ribbons on it there could be asymmetric heating resulting in a lower heat transfer coefficient. It was felt that the error from this discrepancy was less than one per cent. The radiation effect could have introduced an error of about 1 per cent and conduction effects along the ribbon are less than 1 per cent. Summing up all the individual errors, the total error is believed to be not over 6 per cent.

## SECTION VIII

## CONCLUSIONS

Local heat transfer coefficients were studied in detail in one baffle space of a model segmental baffled tubular heat exchanger. Two baffle spacings and three flow rates were investigated for a tube bundle containing 14 tubes in staggered arrangement. Extensive data were obtained for the baffle space and they were processed on the Alwac III E digital computer. They are presented in a picture form for easier interpretation.

The following conclusions are drawn from the data:

1. Correlation of Data

A correlation of the product of the Nusselt number and the Prandtl number versus the weighted Reynolds number was obtained using the equation suggested by Donohue (8) and compared with similar correlations with other investigators, Williams and Katz (35) and Ambrose (1). The present data were in good agreement with those of other workers. The present data were compared with those of Ambrose who used the same apparatus and a good agreement was observed. The findings of Ambrose with respect to:

1. The effect of baffle spacing

2. The effect of clearance between baffle holes and tube.
3. The variation of heat transfer coefficients in the three different flow zones.
4. The variation of heat transfer coefficient along and around a tube

were confirmed by the present study.

## 2. Effect of Baffle Spacing

From the two different baffle spacing studied it was found that smaller baffle spacing definitely results in a higher heat transfer rate. The baffle spacing appear to have a significant effect on the flow pattern but baffle spacings smaller than three quarters of the shell diameter are not very advantageous. This is evident from the reduction of turbulence in the eddy zone to the point that the local heat transfer coefficient is reduced for the smaller baffle spacing (10 baffles) as compared to the larger baffle spacing (6 baffles).

## 3. Effect of Flow Rate

Increase in rate of flow of the shell-side fluid increases the rate of heat transfer. The flow rate has no effect on the effect of the leakage from the clearance between the baffle holes and the tube. It also has little effect on the flow pattern.

The shell-side flow appears to be divided into three zones, longitudinal flow, cross-flow and eddy flow zones. The longitudinal flow occurs in the baffle windows. The cross-flow and eddy flow divide the chamber into two equal parts. The cross-flow is in the downstream half and the eddy flow in the upstream half of the baffle space. The cross-flow forms the main stream from which the eddy flow separates and rejoins. The leakages from the various clearances in the exchanger appear to affect the flow pattern but this effect is only shown qualitatively in the present work. The average heat transfer coefficients for the various zones is shown in Table 8 and Figure 21. It can be seen from Table 8 that the average Nusselt number for a flow rate of 120 cubic feet per minute for the eddy zone is 144.32 for the smaller baffle spacing (10 baffles) and 11.4 per cent higher than the Nusselt number in the cross-flow zone. The average Nusselt number for the longitudinal zone is 131.39. The values for the larger baffle spacing (6 baffles), 120 cubic feet per minute are, for the longitudinal 118.48; for cross-flow 110.41; and for the eddy zone 140.91. In this case the eddy zone coefficient is 27.6 per cent higher than the cross-flow coefficient.

### 5. Heat Transfer Rates Along Tubes

Heat transfer rates along tubes are at a maximum at the baffles and at a minimum at the center of the baffle space. The maximum values decrease by 50 per cent within one inch from the baffle in the exchanger studied. The variation in the space between one baffle and the next baffle is symmetrical with low turbulence in the eddy zone but quite distorted with high turbulence, such as occurs in the eddy flow zones.

### 6. Heat Transfer Around a Tube

The rate of heat transfer varies around a tube with a maximum at the leading edge and a minimum at some other location depending on the pattern of flow in that region. These variations are presented in picture form in Figures 12, 13, 14, 15, 16 and 17, and this permitted mapping the flow pattern shown in Figure 20.

## SECTION IX

## RECOMMENDATIONS

The study of Ambrose (1) to understand the shell-side characteristics of a baffled tubular heat exchanger were exploratory in nature. In the present investigation two aspects, the effect of baffle spacing and flow rate, were studied. This work also consisted of detailed examination of the flow pattern in the vicinity of baffles. It indicated that more needs to be done to completely understand the effect of the various clearances in the exchanger. It also recommended that a study with more flow rates will help substantiate the present findings. A more detailed study at the entrance and exit of the shell will give a more complete picture of the entire heat exchanger.

The effect of different tube spacings and tube sizes merits investigation.



## SECTION X

## NOMENCLATURE

- A Area of surface, square feet;  $A_{av}$ , average area;  $A_b$ , baffle window area;  $A_c$ , cross flow area in tube bank;  $A_s$ , shell-side;  $A_t$ , tube-side;  $A_w$ , baffle window area.
- B Baffle height, feet.
- $C_p$  Specific heat at a constant pressure, Btu/(lb) (deg. F).
- C Specific heat of fluid Btu/(lb) (deg. F).
- D Diameter of heat exchanger shell, feet.
- $D_e$  Equivalent diameter  $\frac{4 \text{ (flow area)}}{\text{wetted perimeter}}$ , inches
- d Diameter of tube, feet;  $d_i$ , inside tube diameter.
- G Mass velocity, lbs/(hr) (sq. ft.);  $G_e$ , weighted;  $G_s$ , shell-side.
- H Differential manometer reading, inches.
- h Heat transfer coefficient, Btu/hr. (sq. ft.) (deg. F);  $h_{av}$ , average of local coefficients around tube;  $h_o$ , for natural convection;  $h_{as}$ , for scale on shell-side;  $h_{at}$ , for scale on tube-side;  $h_s$ , for film on shell-side;  $h_t$ , for film on tube-side,  $h_o$ , heat transfer coefficient for outside fluid.
- i Current, amperes.
- $j_h$  Heat transfer j-factor (defined on p. 29).
- $j_m$  Mass transfer j-factor (defined on p. 29).
- K Molar mass-transfer coefficient, lb. mols/(hr) (sq. ft.) (atm).

- k Thermal conductivity, Btu/(hr) (sq. ft.) (deg. F)/ft;  
 $k_w$ , for tube wall.
- L Active length of heat exchanger, feet
- M Molecular weight of air.
- mv Millivolts.
- Nu Nusselt number  $\frac{hd}{k}$ , dimensionless.
- P Tube pitch (distance between centers of heat exchanger tubes), feet
- Pr Prandtl number  $\frac{C_p \mu}{k}$ , dimensionless.
- p Pressure, lbs/(sq in).
- Q Flow rate of air, cu ft/min.
- q Heat transfer rate, Btu/hr.
- R Resistance of ribbon. Ohms/ft.
- Re Reynolds number  $\frac{d V \rho}{\mu}$ , dimensionless
- r Radius, inches
- S Baffle spacing, feet.
- St Stanton number  $\frac{h}{G C_p}$ , dimensionless.
- T Temperature, deg. Rankine;  $T_a$ , air temperature
- t Temperature, deg. F;  $t_a$ , air temp;  $t_f$ , fluid temp;  
 $t_s$ , surface temp.
- U Over-all heat transfer coefficient, Btu/(hr) (sq ft)  
(deg. F).
- V Velocity, ft/hr.
- W Width of resistance ribbon, inches.
- w Mass flow rate, lbs/hr.

- X Code letter indicating 2 3/16-inch tube pitch.
- x Horizontal distance, feet;  $x_b$ , distance between baffles, inches.
- Y Code letter indicating 1 1/4-inch tube pitch.
- Z Thickness of resistance ribbon, inches.
- $\alpha$  Proportionality constant.
- $\epsilon$  Emissivity, dimensionless.
- $\theta$  Angle measured from the leading edge, degrees.
- $\mu$  Viscosity, lb/(sq ft) (hr);  $\mu_w$ , viscosity at the wall.
- $\rho$  Density, lb/cu ft;  $\rho_E$ , or exchanger;  $\rho_o$ , at orifice.
- $\sigma$  Stefan-Boltzmann constant, Btu/(hr) (sq ft) (deg.R)<sup>4</sup>.

## SECTION XI

## BIBLIOGRAPHY

1. Ambrose, Tommy W. Local shell-side heat transfer coefficients in baffled tubular heat exchangers. Ph.D. Thesis. Corvallis, Oregon State College, 1957. 183 numb. leaves.
2. Bergelin, O. P., G. A. Brown and S. C. Doberstein. Heat transfer and fluid friction during flow across banks of tubes. IV. Transactions of the American Society of Mechanical Engineers 74:953-960. 1952.
3. Bergelin, O. P., G. A. Brown and A. P. Colburn. Heat transfer and fluid friction during flow across banks of tubes. V. Transactions of the American Society of Mechanical Engineers 76:841-850. 1954
4. Breindenbach, E. P., and H. E. O'Connel. Predicting commercial heat transfer coefficients. Transactions of the American Institute of Chemical Engineers 42:761-776. 1946.
5. Colburn, A. P. A method of correlating forced convection heat transfer data and a comparison with fluid friction. Transactions of the American Institute of Chemical Engineers 29:174-210. 1933.
6. Colburn, A. P., and O. A. Hougen. Measurement of fluid and surface temperatures. Industrial and Engineering Chemistry 22:522. 1930
7. DeBortoli, R. A., R. E. Grimble and J. E. Zerbe. Average and local heat transfer for cross-flow through a tube bank. New York, The American Society of Mechanical Engineers, 1955. 10 p. (The American Society of Mechanical Engineers, Paper No. 55-SA-51)

8. Donohue, Daniel A. Heat transfer and pressure drop in heat exchangers. Industrial and Engineering Chemistry 41 (11): 2499-2511. 1949.
9. Drake, R. M. Jr. Investigation of the variation of point unit heat-transfer coefficients for laminar flow over an inclined flat plate. Journal of Applied Mechanics 16 (1): 1-8. March 1949.
10. Drake, R. M. Jr. et al. Local heat transfer coefficients on the surface of an elliptical cylinder, axis ratio 1:3, in a high speed air stream. New York, The American Society of Mechanical Engineers, 1952. 16 p. (The American Society of Mechanical Engineers. Paper No. 52-A-59)
11. Dwyer, O. E. et al. Heat transfer rates for cross-flow of water through a tube bank at Reynolds numbers up to a million. Upton, Brookhaven National Laboratory, n. d. 23 p. (Brookhaven National Laboratory 1518) (Microcard)
12. Fourier, J. B. J. Theorie analytique de la chaleur. Gauthier Villars. 1888. English translation by A. Freeman. Cambridge, England. 1878.
13. Giedt, W. H. Investigation of variation of point unit heat-transfer coefficient around a cylinder normal to an air stream. Transaction of the American Society of Mechanical Engineers 71:375-381. 1949.
14. Grimison, E. D. Correlation and utilization of new data on flow resistance and heat transfer for cross flow of gases over tube banks. Transactions of the American Society of Mechanical Engineers 59:583-94. 1937.
15. Gunter, A. Y., H. R. Sennstrom and S. Kopp. A study of flow patterns in baffled heat exchangers. Paper presented at the annual meeting of the American Society of Mechanical Engineers, Atlantic City, New Jersey. December, 1947.

16. Gupta, Rajeshwar K and Donald L. Katz. Use of flow patterns in predicting shell-side heat transfer coefficients for baffled shell-and-tube exchangers. Paper presented at the Industrial and Engineering Chemistry Symposium on Fluid Mechanics in Chemical Engineering, Purdue University, Lafayette, Indiana. December 27-28, 1956.
17. Kays, W. M., A. L. London and R. K. Lo. Heat transfer and friction characteristics for gas flow normal to tube banks --use of a transient test technique. Transactions of the American Society of Mechanical Engineers 76:387-396. 1954.
18. Kern, Donald Q. Process heat transfer. New York, McGraw-Hill, 1950. 871 p.
19. Knudsen, James G. and Donald L. Katz. Fluid dynamics and heat transfer. 1957. (In press)
20. Leeds and Northrup Company, Electrical Measuring Instruments. Standard conversion tables for L and N thermocouples. Philadelphia, Leeds and Northrup Company, n. d. 43 p. (Leeds and Northrup Company, Standard 31031)
21. Levy, Solomon. Heat transfer to constant-property laminar boundary-layer flows with power-function free-stream velocity and wall-temperature variation. Journal of the Aeronautical Sciences 19:341-348. 1952
22. McAdams, Williams H. Heat transmission. 3rd ed. New York, McGraw-Hill, 1954. 532 p.
23. Martinelli, R. C. et al. An investigation of aircraft heaters. VIII A simplified method for the calculation of the unit thermal conductance over wings. Washington, 1943. 16 p. (National Advisory Committee for Aeronautics. War Report 14)
24. Milne, William Edmund. Numerical calculus. Princeton, Princeton University Press, 1949. 393 p.

25. Perrone, S. A. Pressure drop and heat transfer in exchangers. The Oil and Gas Journal 33:71-76. March 28, 1935.
26. Schmidt, Ernst and Karl Wenner. Heat transfer over the circumference of a heated cylinder in transverse flow. Washington 1943. 15 p. (National Advisory Committee for Aeronautics. Technical Memorandum No. 1050)
27. Short, B. E. A review of heat transfer coefficients and friction factors in tubular heat exchangers. Transactions of the American Society of Mechanical Engineers 64:779-785. 1942.
28. Short, B. E. Heat transfer and pressure drop in heat exchangers. Austin, The University of Texas, 1943. 55 p. (University of Texas. Bureau of Engineering Research. Bulletin No. 4324)
29. Simonds, Herbert R., Archie J. Weith and M. H. Bigelow. Handbook of plastics. 2d ed. New York, Van Nostrand, 1949. 1511 p.
30. Snyder, N. W. Heat transfer in air from a single tube in a staggered-tube bank. In: American Institute of Chemical Engineers' Chemical Engineering Progress Symposium series Vol. 49. No. 5. New York, 1953. p. 11-20.
31. Thomson, A. S. T. et al. Variation in heat transfer rates around tubes in cross flow. In: The Institution of Mechanical Engineers and The American Society of Mechanical Engineers' proceedings of the general discussion on heat transfer, Sept. 11-13, 1951. London, Institution of Mechanical Engineers, 1952. p. 177-180.
32. Tinker, Townsend. Shell side characteristics of shell and tube heat exchangers. Part I Analysis of the fluid flow pattern in shell and tube heat exchangers and the effect of flow distribution on the heat exchanger performance. In: The Institution of Mechanical Engineers and the American

Society of Mechanical Engineers' proceedings of the general discussion on heat transfer, Sept. 11-13, 1951. London, Institution of Mechanical Engineers, 1952. p. 89-96.

33. Tinker, Townsend. Shell side characteristics of shell and tube heat exchangers. Part II A co-ordination of the test performance of several shell and tube heat exchangers on the basis of "effective flow areas" calculated from the dimensional characteristics and mechanical clearances of the exchangers. In: The Institution of Mechanical Engineers and The American Society of Mechanical Engineers' proceedings of the general discussion on heat transfer, Sept. 11-13, 1951. London, Institution of Mechanical Engineers, 1952. p. 97-109.
34. Tinker, Townsend. Shell side characteristics of shell and tube heat exchangers. Part III A quantitative analysis of the effect of dimensional characteristics and mechanical clearance on the shell side performance of a typical shell and tube heat exchanger. In: The Institution of Mechanical Engineers and the American Society of Mechanical Engineers proceedings of the general discussion on heat transfer, Sept. 11-13, 1951. London, Institution of Mechanical Engineers, 1952. p. 110-116.
35. Williams, Richard B. and Donald L. Katz. Performance of finned tubes in shell and tube heat exchangers. Ann Arbor, University of Michigan, 1951. 154 p. (University of Michigan. Engineering Research Institute. Project M592)
36. Winding, C. C. and A. J. Cheney, Jr. Mass and heat transfer in tube banks. Industrial and Engineering Chemistry 40:1087-1093. 1948.
37. Zapp, George Michael, Jr. The effect of turbulence on local heat transfer coefficients around a cylinder normal to an air stream. Master's thesis. Corvallis, Oregon State College, 1950. 79 numb. leaves.



## APPENDIX

# Summary of Equations Used to Compute the Local Heat Transfer Coefficients

Equation 14 was used to convert millivolts to temperature units.

$$t = -0.26 (\text{mv})^2 + 35.12 (\text{mv}) + 32.01 \quad (14)$$

The first temperature derivatives were calculated by equation 20.

$$\begin{aligned} \frac{dt_1}{d\theta} &= \frac{1}{2h} \left( -3t_1 + 4t_2 - t_3 \right) \\ \frac{dt_2}{d\theta} &= \frac{1}{2h} \left( -t_1 + t_3 \right) \\ &\vdots \\ \frac{dt_7}{d\theta} &= \frac{1}{2h} \left( t_5 - 4t_6 + 3t_7 \right) \end{aligned} \quad (20)$$

Equation 21 was used to calculate the second derivatives.

$$\begin{aligned} \frac{d^2 t_1}{d\theta^2} &= \frac{1}{2h} \left( -3 \frac{dt_1}{d\theta} + 4 \frac{dt_2}{d\theta} - \frac{dt_3}{d\theta} \right) \\ &\vdots \\ \frac{d^2 t_2}{d\theta^2} &= \frac{1}{2h} \left( -\frac{dt_1}{d\theta} + \frac{dt_3}{d\theta} \right) \\ &\vdots \\ \frac{d^2 t_7}{d\theta^2} &= \frac{1}{2h} \left( \frac{dt_5}{d\theta} - 4 \frac{dt_6}{d\theta} + 3 \frac{dt_7}{d\theta} \right) \end{aligned} \quad (21)$$

The local heat transfer coefficients were calculated using equation 13a.

$$h = \frac{11.10 \, i^2 + 2404 \, \frac{d^2 t}{d\theta^2}}{t - t_a} \quad \begin{matrix} 86 \\ (13a) \end{matrix}$$

The average heat transfer coefficient at a position was calculated using equation 15

$$h_{av} = \frac{1}{7} \sum_1^7 h \quad (15)$$

Equation 16 was used to calculate the Nusselt number at a position

$$Nu = \frac{h_{av} d}{k} \quad (16)$$

where  $k$  was calculated from equation 17.

$$k = 0.0000245 \, t_a + 0.132 \quad (17)$$

These equations are quoted from Ambrose (1).

E Eddy Zone  
L Longitudinal Zone  
C Cross Flow Zone

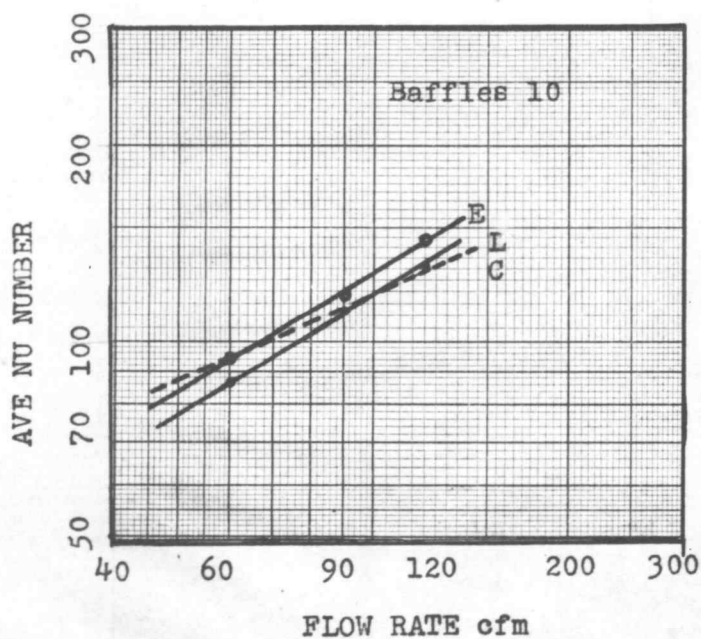
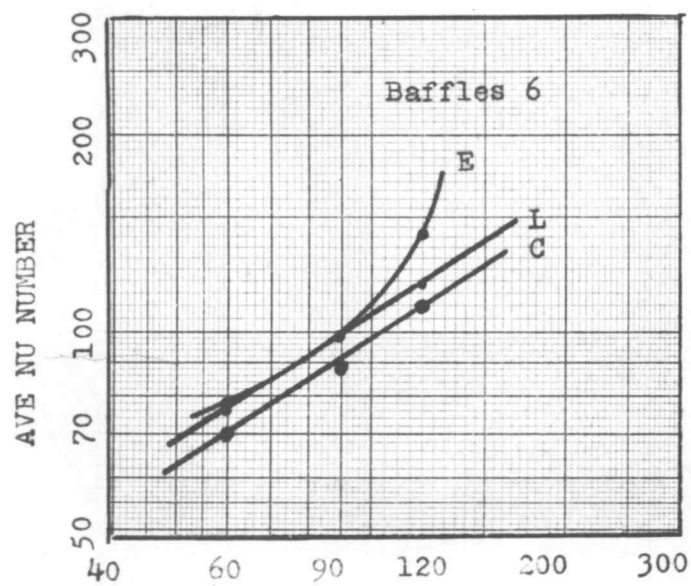


FIGURE 21 VARIATION OF NUSSELT NUMBERS WITH FLOW RATE

## PROGRAM

The program used for calculating the data is given in page 89. The first three paragraphs refer to the calculation of the local temperatures, local heat transfer coefficients, average heat transfer coefficients and average Nusselt numbers. The order of input of data is

1	2	3	4	5	6	7	8	9
Millivolt readings								Current in amperes

The next two paragraphs refer to the calculation of air flow rates. The order of input of data is

1	2	3	4
$P_o$	T	$P_E$	K

where

$P_o$	pressure at the orifice, psig
T	Temperature, $^{\circ}F$
$P_E$	pressure at the exchanger, psig
K	Constant obtained from a chart of Ambrose(1)

40 1

00	8341	5703	80	01	3000	e648	81	02	411f	e749	82	03	0009	0000	83
04	871e	2800	84	05	a30c	6117	85	06	a304	614b	86	07	0014	008c	87
08	f782	5b07	88	09	4848	4851	89	0a	495f	411e	8a	0b	0008	0000	8b
0c	1160	4849	8c	0d	5b1b	871f	8d	0e	e74a	a304	8e	0f	428f	5c28	8f
10	1784	790d	90	11	1160	2800	91	12	675f	4950	92	13	0231	eb85	93
14	f781	570b	94	15	f781	1718	95	16	5727	1120	96	17	0200	28f5	97
18	410f	e648	98	19	790d	f781	99	1a	0002	0000	9a	1b	0314	0291	9b
1c	6713	2e00	9c	1d	571a	c323	9d	1e	4000	0000	9e	1f	3000	0000	9f

41 2

20	7850	664e	a0	21	4850	17bc	a1	22	495f	7847	a2	23	0000	0000	a3
24	4856	1720	a4	25	5723	179d	a5	26	6747	3a00	a6	27	0005	0000	a7
28	411e	e74e	a8	29	4133	e748	a9	2a	795f	a10c	aa	2b	0007	0000	ab
2c	a304	495f	ac	2d	a30c	3000	ad	2e	e900	332c	ae	2f	4bfa	6df0	af
30	411f	e74f	b0	31	e748	a30c	b1	32	4847	5b3b	b2	33	00b1	999a	b3
34	a304	614d	b4	35	4948	572b	b5	36	1160	2800	b6	37	5b00	0000	b7
38	675f	4956	b8	39	8142	412f	b9	3a	f781	17b9	ba	3b	0314	02b6	bb
3c	572b	7857	bc	3d	e657	6148	bd	3e	1180	0000	be	3f	8140	1100	bf

42 3

40	0000	572b	c0	41	0000	4907	c1	42	113f	0000	c2	43	0070	0000	c3
44	2930	2800	c4	45	4113	e747	c5	46	0000	0000	c6	47	0000	0000	c7
48	6047	1708	c8	49	6117	3a00	c9	4a	0000	0000	ca	4b	158b	f267	cb
4c	a10c	eb03	cc	4d	2930	7907	cd	4e	0000	0000	ce	4f	0314	0218	cf
50	c507	3200	d0	51	a10c	e900	d1	52	0000	0000	d2	53	0001	9b0b	d3
54	5b0f	1160	d4	55	3200	5b1b	d5	56	0000	0000	d6	57	0000	3611	d7
58	2800	f781	d8	59	1160	791f	d9	5a	0000	0000	da	5b	0314	0299	db
5c	410b	e707	dc	5d	f781	f781	dd	5e	0000	0000	de	5f	5b68	0000	df

60 1

00	8361	871e	80	01	4060	1705	81	02	e660	eb0b	82	03	0000	0000	83
04	571f	c313	84	05	7860	610f	85	06	c503	c33c	86	07	0095	0000	87
08	571b	5b17	88	09	3a00	e500	89	0a	2800	792d	8a	0b	001a	4dd2	8b
0c	1160	4860	8c	0d	a108	c303	8d	0e	673c	4d1a	8e	0f	1cc0	0000	8f
10	1788	5713	90	11	8705	5b07	91	12	5721	871f	92	13	0000	0000	93
14	8c60	1784	94	15	1160	5703	95	16	0000	5b29	96	17	0014	008c	97
18	571f	c313	98	19	1799	a308	99	1a	7800	1160	9a	1b	0020	0000	9b
1c	8460	571b	9c	1d	ea60	1702	9d	1e	2800	1120	9e	1f	0002	0000	9f

61 2

20	f701	1796	a0	21	0004	0000	a1	22	0000	0000	a2	23	0000	0000	a3
24	2800	f701	a4	25	0314	02ac	a5	26	0000	0000	a6	27	0000	0000	a7
28	5b25	7903	a8	29	0314	021e	a9	2a	0000	0000	aa	2b	0000	0000	ab
2c	1160	7928	ac	2d	0061	0000	ad	2e	0000	0000	ae	2f	0000	0000	af
30	f701	573c	b0	31	0000	0000	b1	32	0000	0000	b2	33	0000	0000	b3
34	1701	5713	b4	35	0000	0000	b5	36	0000	0000	b6	37	0000	0000	b7
38	1798	1100	b8	39	0000	0000	b9	3a	0000	0000	ba	3b	0000	0000	bb
3c	0000	0000	bc	3d	0000	0000	bd	3e	0000	0000	be	3f	0000	0000	bf

TABLE 3

## Calculated Data for Correlation

Number of Baffles	$A_c \text{ ft.}^2$	$A_b \text{ ft.}^2$	$\sqrt{A_c A_b}$ $\text{ft.}^2$	$G_e$ lbs/hr.ft	Reynolds Number $\frac{G_e d}{\mu}$	Nusselt Number $\frac{h d}{k}$	$(Nu)(Pr)^{-1/3}$
6	0.0753	0.0343	0.0508	5232.87	10,013.1	72.80	82.15
6	0.0753	0.0343	0.0508	8,048.8	15,401.5	95.04	107.25
6	0.0753	0.0343	0.0508	10,471.9	20,038.3	123.62	139.51
10	0.0474	0.0343	0.0403	6,596.3	12,622.0	91.36	103.10
10	0.0474	0.0343	0.0403	10,114.4	19,353.9	113.18	127.72
10	0.0474	0.0343	0.0403	13,392.4	25,626.5	135.36	152.75

\* In all the above calculations a constant value of 0.7 was used for Prandtl number for air.

TABLE 4

Calculated Average Flow Rates

Number of Baffles 6

Tube Number	Investigation Position Number										
	1	2	3	4	5	6	7	8	9	10	11
L	59.28	59.28	59.28	59.28	59.28	59.28	59.28	59.28	59.28	59.28	59.28
2	59.32	59.32	59.32	59.32	59.32	59.32	59.32	59.32	59.32	59.32	59.32
3	58.47	58.47	58.47	58.47	58.47	58.47	58.47	58.47	58.47	58.47	58.47
4	59.07	59.07	59.07	59.07	59.07	59.07	59.07	59.07	59.13	59.13	59.13
5	59.25	59.25	59.25	59.25	59.25	59.25	59.25	59.25	59.25	59.25	59.25
6	60.10	60.10	60.10	60.10	60.10	60.10	60.10	60.10	60.10	60.10	60.10
7	59.33	59.33	59.33	59.33	59.33	59.33	59.33	59.33	59.33	59.33	59.33
8	59.33	59.33	59.33	59.33	59.33	59.33	59.33	59.33	59.33	59.33	59.33
9	59.33	59.33	59.33	59.33	59.33	59.33	59.33	59.33	59.33	59.33	59.33
10	59.40	59.40	59.40	59.40	59.40	59.40	59.40	59.40	59.40	59.40	59.40
11	59.40	59.40	59.40	59.40	59.40	59.40	59.40	59.40	59.40	59.40	59.40
12	59.40	59.40	59.40	59.40	59.40	59.40	59.40	59.40	59.40	59.40	59.40
13	54.54	54.54	54.54	54.54	54.54	54.54	54.54	54.54	54.54	54.54	54.54
14	54.53	54.53	54.53	54.53	54.53	54.53	54.53	54.53	54.53	54.53	54.53
1	90.40	90.40	90.40	90.40	90.40	90.40	90.40	90.40	90.40	90.40	90.40
2	89.92	89.92	89.92	89.92	89.92	89.92	89.92	89.92	89.92	89.92	89.92
3	90.40	90.40	90.40	90.40	90.40	90.40	90.40	90.40	90.40	90.40	90.40
5	91.04	91.04	91.04	91.04	91.04	91.04	91.04	91.04	91.04	91.04	91.04
6	91.11	91.11	91.11	91.11	91.11	91.11	91.11	91.11	91.11	91.11	91.11
7	90.71	90.71	90.71	90.71	90.71	90.71	90.71	90.71	90.71	90.71	90.71



TABLE 4

Tube Number	1	2	3	4	5	6	7	8	9	10	11
8	90.54	90.54	90.54	90.54	90.54	90.54	90.54	90.54	90.54	90.54	90.54
9	90.27	90.27	90.27	90.27	90.27	90.27	90.27	90.27	90.27	90.27	90.27
10	90.45	90.45	90.45	90.45	90.45	90.45	90.45	90.45	90.45	90.45	90.45
11	90.45	90.45	90.45	90.45	90.45	90.45	90.45	90.45	90.45	90.45	90.45
12	90.72	90.72	90.72	90.72	90.72	90.72	90.72	90.72	90.72	90.72	90.72
13	89.20	89.20	89.20	89.20	89.20	89.20	89.20	89.20	89.20	89.20	89.20
14	89.54	89.54	89.54	89.54	89.54	89.54	89.54	89.54	89.54	89.54	89.54
1	118.84	118.84	118.84	118.84	118.84	118.84	118.84	118.84	118.84	118.84	118.84
2	119.31	119.31	119.31	119.31	119.31	119.31	119.31	119.31	119.31	119.31	119.31
3	119.98	119.98	119.98	119.98	119.98	119.98	119.98	119.98	119.98	119.98	119.98
4	119.74	119.74	119.74	119.74	119.74	119.74	119.74	119.74	119.74	119.74	119.74
5	120.28	120.28	120.28	120.28	120.28	120.28	120.28	120.28	120.28	120.28	120.28
6	119.75	119.75	119.75	119.75	119.75	119.75	119.75	119.75	119.75	119.75	119.75
7	120.00	120.00	120.00	120.00	120.00	120.00	120.00	120.00	120.00	120.00	120.00
8	120.00	120.00	120.00	120.00	120.00	120.00	120.00	120.00	120.00	120.00	120.00
9	119.31	119.31	119.31	119.31	119.31	119.31	119.31	119.31	119.31	119.31	119.31
10	119.31	119.31	119.31	119.31	119.31	119.31	119.31	119.31	119.31	119.31	119.31
11	119.31	119.31	119.31	119.31	119.31	119.31	119.31	119.31	119.31	119.31	119.31
12	119.31	119.31	119.31	119.31	119.31	119.31	119.31	119.31	119.31	119.31	119.31
13	117.50	117.50	117.50	117.50	117.50	117.50	117.50	117.50	117.50	117.50	117.50
14	117.50	117.50	117.50	117.50	117.50	117.50	117.50	117.50	117.50	117.50	117.50

TABLE 5

Calculated Average Flow Rates

Number of Baffles 10

Tube Number	Investigation Position Number						
	1	2	3	4	5	6	7
1	58.08	58.07	58.08	58.07	57.69	59.62	59.62
2	58.67	58.67	58.67	58.62	58.44	58.63	58.63
3	58.80	58.80	58.80	58.80	58.80	58.80	58.80
4	59.17	59.17	59.17	59.17	59.17	59.17	59.17
5	59.33	59.33	59.33	59.33	59.33	59.33	59.33
6	58.92	58.92	58.92	58.92	58.92	58.92	58.92
7	59.02	59.02	59.02	59.02	59.02	59.02	59.02
8	58.60	58.60	58.60	58.60	58.60	58.60	58.60
9	58.60	58.60	58.60	58.60	58.60	58.60	58.60
10	58.65	58.65	58.65	58.65	58.65	58.65	58.65
11	58.84	58.84	58.84	58.84	58.84	58.84	58.84
12	59.09	59.09	59.09	59.09	59.09	59.09	59.09
13	58.77	58.77	58.77	58.77	58.77	58.77	58.77
14	59.28	59.28	59.28	59.28	59.28	59.28	59.28
1	90.40	90.40	90.40	90.40	90.40	90.40	90.40
2	89.92	89.92	89.92	89.92	89.92	89.92	89.92
3	90.40	90.40	90.40	90.40	90.40	90.40	90.40
4	90.64	90.64	90.64	90.64	90.64	90.64	90.64
5	91.04	91.04	91.04	91.04	91.04	91.04	91.04
6	91.11	91.11	91.11	91.11	91.11	91.11	91.11
7	90.71	90.71	90.71	90.71	90.71	90.71	90.71

TABLE 5

Tube Number	1	2	3	4	5	6	7
8	90.54	90.54	90.54	90.54	90.54	90.54	90.54
9	90.27	90.27	90.27	90.27	90.27	90.27	90.27
10	90.45	90.45	90.45	90.45	90.45	90.45	90.45
11	90.45	90.45	90.45	90.45	90.45	90.45	90.45
12	90.72	90.72	90.72	90.72	90.72	90.72	90.72
13	89.20	89.20	89.20	89.20	89.20	89.20	89.20
14	89.54	89.54	89.54	89.54	89.54	89.54	89.54
1	117.28	117.28	117.28	117.28	117.28	117.28	117.28
2	115.42	115.42	115.42	115.42	115.42	115.42	115.42
3	116.77	116.77	116.77	116.77	116.77	116.77	116.77
4	117.68	117.68	117.68	117.68	117.68	117.68	117.68
5	118.15	118.15	118.15	118.15	118.15	118.15	118.15
6	118.15	118.15	118.15	118.15	118.15	118.15	118.15
7	117.76	117.76	117.76	117.76	117.76	117.76	117.76
8	117.91	117.91	117.91	117.91	117.91	117.91	117.91
9	117.91	117.91	117.91	117.91	117.91	117.91	117.91
10	117.76	117.76	117.76	117.76	117.76	117.76	117.76
11	117.76	117.76	117.76	117.76	117.76	117.76	117.76
12	118.02	118.02	118.02	118.02	118.02	118.02	118.02
13	118.02	118.02	118.02	118.02	118.02	118.02	118.02
14	117.76	117.76	117.76	117.76	117.76	117.76	117.76

TABLE 6

Variation of Average Nusselt Numbers With Flow Rate

Number of Baffles	Baffle Spacing inches	Average Rate of Flow cfm	Average Nusselt Number	Per Cent Increase of Nu Number for 10 Baffles over 6 Baffles	Per Cent Increase of Nu Number over 60 cfm Flow Rate
6	6.43	58.65	72.80	-	-
6	6.43	90.39	95.04	-	30.55
6	6.43	119.30	123.62	-	73.35
10	4.09	58.73	91.36	25.5	-
10	4.09	90.38	113.18	19.1	23.88
10	4.09	117.60	135.36	9.1	48.16

TABLE 7

## Effect of Baffle Hole Clearance

Number of Baffles	Flow Rate cfm	High value of Nu Number	Low value of Nu Number *	Per Cent Increase of High Value over the Low Value
6	58.65	72.80	60.13	21.07
6	90.39	95.04	78.91	20.44
6	119.30	123.62	98.42	25.60
10	58.73	91.36	79.04	15.59
10	90.38	113.18	98.56	14.83
10	117.60	135.36	118.30	14.42

\* The low values were obtained by neglecting one value on each baffle in the case of 10 baffles and two values at each baffle in the case of 6 baffles.

TABLE 8

## Average Nusselt Numbers in the Various Flow Zones

Number of Baffles	Rate of Flow cfm	Average Nusselt Numbers				Overall
		Longitudinal Flow Zone	Cross-Flow Zone	Eddy Zone	Per Cent Incr- ease in Eddy Zone over Cr. Flow Zone	
6	58.65	75.82	70.07	77.83	11.11	72.80
6	90.39	98.90	89.12	98.44	10.50	95.04
6	119.30	118.48	110.41	140.91	27.60	123.62
10	58.73	86.75	92.56	93.83	1.37	91.36
10	90.38	110.49	110.51	118.02	6.80	113.18
10	117.60	131.39	129.55	144.32	11.40	135.36